Chair of Geology and Economic Geology

Master's Thesis

A contribution of Middle – Late Jurassic Mélanges in the Northern Calcareous Alps (Raucherschober/Schafkogel) and the Inner Western Carpathians (Jaklovce) to the reconstruction of the Triassic – Jurassic passive and active Neo-Tethys distal continental margin

Sebastian Paul Drvoderic, BSc

May 2021

MONTANUNIVERSITÄT LEOBEN
www.unileoben.ac.at

EIDESSTATTLICHE ERKLÄRUNG

Ich erkläre an Eides statt, dass ich diese Arbeit selbständig verfasst, andere als die angegebenen Quellen und Hilfsmittel nicht benutzt, und mich auch sonst keiner unerlaubten Hilfsmittel bedient habe.

Ich erkläre, dass ich die Richtlinien des Senats der Montanuniversität Leoben zu "Gute wissenschaftliche Praxis" gelesen, verstanden und befolgt habe.

Weiters erkläre ich, dass die elektronische und gedruckte Version der eingereichten wissenschaftlichen Abschlussarbeit formal und inhaltlich identisch sind.

Datum: 10.05.2021

Unterschrift Verfasser/in
Sebastian Paul Drvoderic

DANKSAGUNG

I would like to thank Ao.Univ.-Prof. Mag. et Dr.rer.nat. Hans-Jürgen Gawlick for supporting this master´s thesis in field work and data processing and Dr. Hisashi Suzuki (university Otani – Yapan) for age determinations of the radiolarians, as well as Dr. Felix Schlagintweit, for microfossil determinations. I also want to say thank you to the whole Department for Applied Geology for the provision of equipment and analysis devices. I do not want to miss the opportunity to thank my family for their support in all the years of my education and especially during my time at Montanuniversität. Finally, I say thank you to B. Steiner for the great support all around this study and more.

Kurzfassung

Mélangen können grundlegende Erkenntnisse zu offenen Fragen der geodynamischen Entwicklung, paläogeographischen Rekonstruktionen und der von Gebirgen liefern. In dieser Studie steht die Rekonstruktion des passiven und aktiven Kontinentalrandes des westlichen Tethys-Raumes von der Mittel-Trias bis ins Mittel Jura im Mittelpunkt. Zwei Mélangen 1) in den Inneren West-Karpaten und 2) den Nördlichen Kalkalpen wurden zu diesem Zweck eingehend untersucht. Einerseits ein mitteltriassischer Block vom Ozeanboden der Neo-Tethys in der ophiolithischen Meliata Mélange in Jaklovce (innere West-Karpaten) und anderseits eine neu entdeckte Hallstatt Mélange mit basaltischen Komponenten in den südöstlichen Nördlichen Kalkalpen. Dies lieferte weitere neue Daten, um offene Fragen über den Zeitpunkt und der tektonischen Struktur des obduzierten Neo Tethys Ozeans zu lösen.

Die erneute detaillierte Untersuchung des Ozeanbodenblockes mit seiner erhaltenen sedimentären Schichtfolge (Steinmann-Trinität) in der bekannten ophiolitischen Mélange im Gebiet von Jaklovce (Meliata-Einheit der Inneren Westkarpaten) wirft ein neues Licht auf die unterschiedlichen Vorstellungen über das Alter und den Ablagerungsbereich dieser Sedimentgesteine. Massive vulkanische Aschen gehen allmählich in silikatische Tone und Radiolarite über, welche im Hangenden zu mehr karbonatischen Ablagerungen übergehen. Die starke Verkieselung dieser Gesteine macht es allerdings schwierig, aussagekräftige Daten zu erhalten. Dennoch lieferten einige Proben ladinische bis karnische Radiolarienalter. Dieser Basaltblock zeigt deutliche Rekristallisation von Chlorit, Actinolit und Epidot. Der Eisenüberschuss wird durch die Bildung von Magnetit während der Ozeanbodenmetamorphose kompensiert.

Eine bislang unbekannte Hallstatt-Mélange unterhalb des oberjurassischen Plassen-Kalkes des Raucherschober/Schafkogel, nördlich der Mürzalpen-Decke und westlich des Hengstpasses (Nördliche Kalkalpen), enthält ophiolithisches Material des ehemaligen Neo-Tethys Ozeans. Diese Blöcke liegen zusammen mit Blöcken vom distalen passiven Schelf (Hallstätter Kalke) in einer radiolaritisch tonigen Matrix aus dem mittleren bis späten Jura. Frühere Interpretationen der verschiedenen Ablagerungen um den Raucherschober/Schafkogel dagegen sehen dieses Gebiet als nach Norden transportierte (kretazische) Schubmasse der Unterlagernden Decken an. Relikte von ophiolithischem Material zeigen eine frühmagmatische, kalkalkalische Zusammensetzung, welche als Resultat einer beginnenden Obduktion und einer Überschiebung von Ophiolith-Decken interpretiert wird. Die mittel-bathonische bis spät oxfordische Mélange Matrix belegt eine beginnende Ophiolith Obduktion im Mitteljura, anstelle der Vorstellung einer frühkretazischen Obduktion. Darüber hinaus wird die Idee einer ophiolithischen Deckenstapelung anstelle einer einzelnen Ophiolithdecke bevorzugt, der über den Kontinentalrand der Neo-Tethys geschoben wurde. Das kann aus der kalkalkalischen Zusammensetzung des ophiolithischen Materials geschlossen werden, was eine partielle Aufschmelzung erfordert.

In einer Zeit abnehmender Tektonik im späten Jura wurde das Melange-Becken durch den Plassen-Kalk versiegelt, welcher einen typischen Verflachungszyklus Trend zeigt.

Abstract

Mélange analysis can contribute fundamentally to solve open questions of the geodynamic history and paleogeographic reconstructions of mountain ranges. In this study, the reconstruction of the Middle Triassic – Middle Jurassic passive and Middle – early Late Jurassic active margin of the Western-Tethys realm is in focus. Two mélanges 1) the ophiolitic Meliata Mélange (Jaklovce) in the Inner Western Carpathians and 2) the Hallstatt Mélange in the Northern Calcareous Alps (Raucherschober/Schafkogel) are studied. This provides new insights to solve further questions about the timing and the tectonic structure of the obduction of the Neo-Tethys ophiolites.

The re-investigation of a well-known ophiolite block with its sedimentary cover rocks (Steinmann-Trinity) in the ophiolitic mélange in the Jaklovce area (Meliata unit of the Inner Western Carpathians) sheds new light on the depositional area of these sediments. Volcanic ashes gradually turn into siliceous clays and up to more carbonatic sedimentary rocks. In cases total silicification of these rocks makes it even hard to obtain meaningful biostratigraphic data. Nevertheless, radiolarian ages from the Ladinian to the Carnian clearly defining an orientation of the oceanic sediments as an overturned block. Alteration of the basalt blocks clearly show recrystallisation of chlorite, actinolite and epidote. Excess of iron is compensated by the formation of magnetite in the process of ocean floor metamorphism.

Further, a so far unknown Hallstatt mélange below the Late Jurassic Plassen Limestone, north of the Mürzalpen nappe and west of the Hengstpass (Northern Calcareous Alps) contains ophiolitic material of the former Neo-Tethys Ocean together with Late Triassic-Early Jurassic open-marine carbonates deriving from the outer shelf (Hallstatt Limestone facies belt). These blocks rest within a Middle to early Late Jurassic radiolaritic – argillaceous matrix. Therefore, the previous assumption of the investigated area, forming a Cretaceous thrust complex cannot be confirmed. Relics of ophiolitic material show calc-alkaline volcanic arc affinity, defining the rock as the product of an intra oceanic subduction and the formation of an early arc during stacking of the oceanic crust. In this case, a Middle Jurassic onset of ophiolite obduction is favoured instead of a Late Jurassic to Early Cretaceous one. Furthermore, the interpretation of an obducting ophiolitic nappe stack instead of a single ophiolite sheet is preferred.

At a time of decreasing tectonic activity in the Late Jurassic, the mélange basin was sealed by the Plassen Limestone, showing a shallowing-upward trend.

Contents

1 Introduction 2
1.1 Stratigraphy 4
2 Geological overview 7
2.1 Inner Western Carpathians 7
2.1.1 Jaklovce controversies 9
2.2 Northern Calcareous Alps 10
2.2.1 Raucherschober/Schafkogel controversies 10
3 Sampling/Methods 11
4 Results 12
4.1 Jaklovce 12
4.1.1 Sedimentary succession 13
4.1.2 Surrounding 20
4.2 Schafkogel/Raucherschober 22
4.2.1 Components of the mélange 24
4.2.2 Sealing of the mélange 36
5 Interpretation of the results 40
5.1 Jaklovce 40
5.2 Raucherschober/Schafkogel 41
5.3 Comparison with Regional Framework 41
6 Conclusion 44
7 Literature 45

1 Introduction

Remnants of the subducted Neo-Tethys ocean and their sedimentary cover are today preserved within mass transported deposits in the Circum-Pannonian mountain ranges (Eatern Alpes, Western Carpathians, Dinarides), formed during the obduction and the disruption of the former passive continental (Frisch & Gawlick, 2003; Gawlick & Missoni, 2019). Trench-like basins in front of the propagating nappe stack are filled by the erosional products of the advancing nappes. These deep-water basin fills which include blocks of the ocean floor and the continental margin within a younger and fine-grained matrix, showing a coarsening-upward trend. Today these basin fills are present as tectonically dismembered olistostromes, defined as sedimentary mélange (Plašienka, 2012; Festa et al., 2016). For the understanding of the evolution and the reconstruction of mountain ranges, these deposits play an important role and can solve fundamental questions, which are discussed controversially. In this study, two different mélanges many kilometers away from each other, in the Inner Western Carpathians (Jaklovce) and the Northern Calcareous Alps (Raucherschober/Schafkogel) are investigated. To solve fundamental questions about the controversial discussed W-Tethys realm in Mesozoic times the focus is on the ophiolitic components, the sedimentary cover and the mélange matrix.

The Tethys Ocean (Suess, 1901) represents an E – W striking ocean system that reached from E-Asia to E/SE Europe in Triassic to Cenozoic times. In contrast the Alpine Atlantic (=Ligurian-Piemont-Penninic-Vah Ocean; Missoni & Gawlick, 2011a) separated the Adriatic plate (Eastern and Southern Alps, the Western Carpathians, Pelso and Tisza units in the Pannonian realm, the Apennine, the Dinarides/Albanides/Hellenides; Bernoulli et al., 2003; Frisch et al., 2011) from Europe since the Jurassic on and forms the east ward prolongation of the Atlantic Ocean. The Pangea Modell of Carey (1958) predicts a northern Palaeotethys (late Palaeozoic – after genesis of Pangaea – to Early Cretaceous) and a southern Neo-Tethys (Triassic – Neogene), which are separated by the Cimmerian continents (Şengör, 1985). These continental blocks were dismembered by oceanic domains, which all exhibits a slightly different geodynamic history. In Asia, this model works nearly perfect (Şengör, 1985; Ricou, 1995; Şengör, 1997, 2015), but in the Mediterranean area (W-End of the Tethys Ocean) it seems more difficult because of the emplacement of the Alpine Atlantic ocean system and the accompanying disruption of the former passive continental margin since Jurassic times. For this Jurassic to Neogene ocean, the controversial term “Alpine Tethys” is often used in paleogeographic reconstructions (Stampfli & Kozur, 2006; Schmid et al., 2008; Handy et al., 2015; Schmid et al., 2020), what also led to the so called “Tethys question”.

In this case, the paleogeographic reconstruction of the W-Tethyan realm in Mesozoic times is still a controversial debate (Figure 1), which forced several different models (e.g., Haas et al., 1995; Stampfli & Kozur, 2006; Schmid et al., 2008; Missoni & Gawlick, 2011a, 2011b; Robertson, 2012). These models and the resulting controversy is summarized in Schmid et al. (2008, 2020), Gawlick & Missoni (2019).

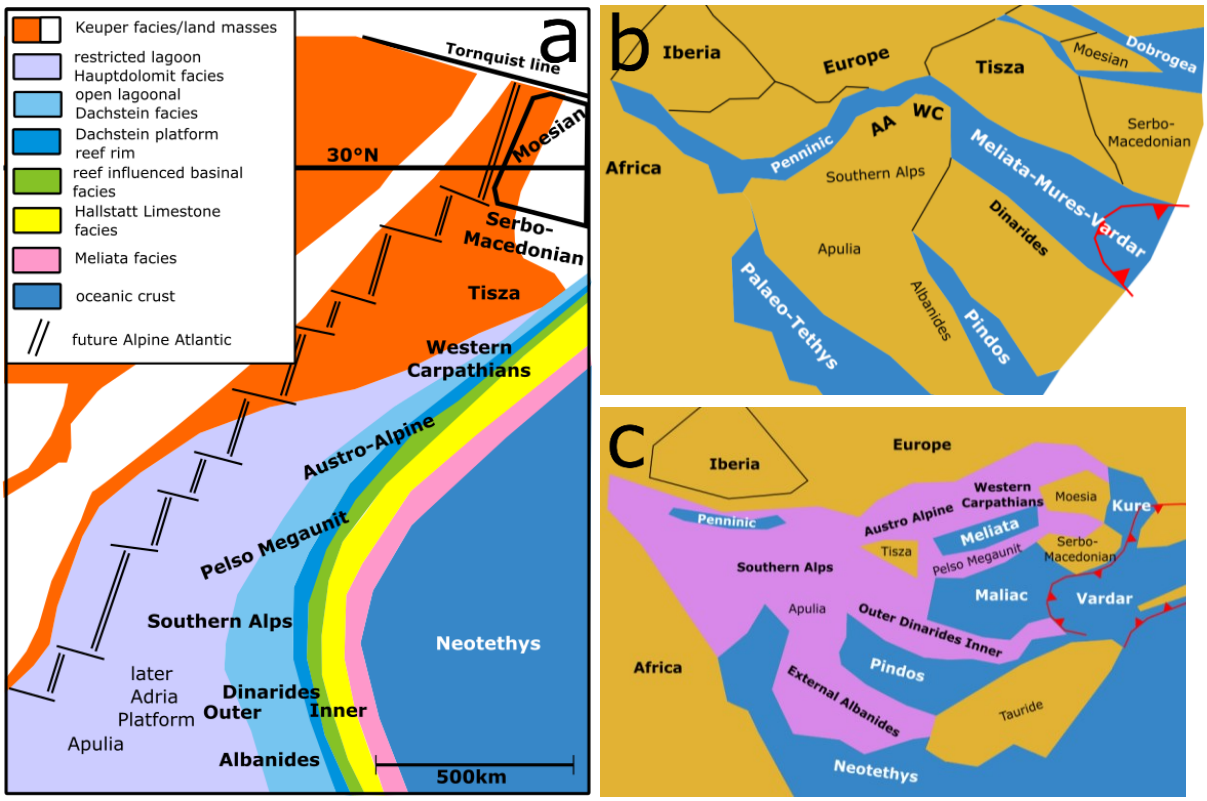

Figure 1: Contrasting palaeogeographic reconstructions of the Western Tethyan realm for the Late Triassic to early Jurassic. a: One-ocean model based on Krystyn and Lein in Haas et al. (1995) in Norian times. b and c: Simplified multi-ocean reconstructions based on b: Csontos & Vörös (2004) in the early Jurassic and c: Stampfli & Kozur (2006).

To come to a reasonable solution a complete reconstruction of the Triassic to Middle Jurassic Neo-Tethys passive continental margin that includes the most distal part and ocean floor is necessary.

The association of red deep-sea clays with radiolarites and Miolica type limestones (Steinmann, 1925, 1927) represent the typical sedimentary cover of the so-called “Steinmann Trinity”, which is characteristic for the depositional environment of the ocean floor (Bernoulli et al., 2003). The relationship between the pillow basalts of the mafic volcanic complex and the sedimentary cover is related to radiolaritic sedimentation within the cavities of the pillow lava, defined as interpillow sedimentation by Pantanelli (1980). He also defined the genetic relationship between these rocks. This knowledge about the integration of oceanic sediments enables a facies integration of similar sediments and a temporal and spacial classification of the rocks. This provides the „missing link“ for a meaningful paleogeographic model. However, such rocks of the oceanic realm are only present in specific geological frameworks, dragged all over the continental margin by obduction. Because of long time tectonic movement which caused destruction of the former ocean floor only leaving its relics behind. Therefore, it is even rarer to obtain a complete succession from the ocean floor and the overlaying sediments, it becomes crucial to investigate these blocks within mass transport deposits and mélanges. In the Northern Calcareous Alps none of these debated Hallstatt mélanges (Gawlick et al., 2007; Missoni & Gawlick, 2011a, 2011b; Gawlick et al., 2012b; Gawlick & Missoni, 2019) contain oceanic crust and even in the Dinarides, such mélanges are not known (Gawlick et al., 2010-Vodena Poljana, Sudar et al., 2010- Pavlovica Cuprija). Only in the Albanides ophiolitic mélanges are existing (Kcira mélange Gawlick et al., 2008, 2014; Gawlick & Missoni, 2019). Such late Middle to early Late Jurassic mélanges (in sense of Frisch & Gawlick, 2003) may play an important role to solve fundamental questions of geodynamic reconstruction of mountain ranges.

Furthermore, the question about the timing of ophiolite obduction arises, also led to different theories from various authors. Due to the obtained mélange ages, the idea of (A) an early Middle Jurassic nappe stacking (Gawlick & Missoni, 2019) contrasts the model of (B) a higher Jurassic to early Cretaceous tectonic movement (Schmid et al., 2008, 2020; Nitra et al., 2020). It is still questioned if Middle to early Late Jurassic ophiolitic mélanges formed in the frame of ophiolite obduction improve a Middle Jurassic onset of obduction, even if they contain continental-derived blocks (Gawlick et al., 2016a). Also the occurrence of Cr-spinels in Kimmeridgian sedimentary rocks (Gawlick et al., 2015) in the Northern Calcareous Alps or in Callovian radiolarites in the Hellenides (Chiari et al., 2013) is not accepted for an early onset of ophiolite obduction by e.g. Nitra et al. (2020) and Schmid et al. (2020).

All these questions about the nappe structure of the obducted ophiolites led to contradicting models. Today, two different models are in contrast to each other: (A) a single thrust sheet was obducted (Schmid et al., 2008) and (B) multiple stacked ophiolites were obducted onto the Neo-Tethys margin (Gawlick et al., 2008).

To solve the questions about the appearance of different ocean systems, the tectonic conditions and the timing of ophiolite obduction, it is necessary to understand the sedimentary conditions at the Neo-Tethys continental margin even before obduction and mountain building to avoid interpretations that lack in knowledge about these starting conditions. The theory that similar rocks are formed in similar geological environments, corresponding to the same ocean system is used to reconstruct parts of the distal Neo-Tethys continental margin to provide a meaningful model of the time before obduction. The focus of this work is on the basaltic rocks of the former ocean crust and the sedimentary cover. They provide meaningful data about the building conditions and the time of formation. Therefore, areas of difficulty and unclearness, which are often interpreted differently (Meliata/Jaklovce) are re-visited and new areas of interest (Raucherschober/Schafkogel) are explored.

1.1 Stratigraphy

The knowledge about the integration of rocks into a specific facies belt and the correlation with processes that effect the sedimentation conditions of the continental margin is necessary to avoid wrong interpretations about structures and lifetime of oceanic domains. Therefore, the stratigraphy of the Neo-Tethys facies belts in Triassic and Jurassic times is crucial to correlate new obtained data (see Figure 2).

From the Late Permian on, siliciclastic sedimentation dominated in the early rift stadium of the Neo-Tethys Wilson-Cycle. Intense carbonate production started around the Early/Middle Triassic boundary with the formation of carbonate ramps. After the Pelsonian drowning event the carbonate production decreased dramatically. This is also related to the ongoing oceanic break-up. The final break-up of the Neo-Tethys Ocean in the Late Anisian (Gawlick et al., 2008; Ozsvart et al., 2012; Sudar et al., 2013) forced deposition of volcanics especially in the most distal passive continental margin setting (Haas et al., 2011 with references therein). Open-marine sediments were deposited from Late Anisian to Late Ladinian practically all over the shelf (see Figure 2). The most distal facies zone (Meliata facies zone) is characterised by the deposition of massive volcanic ashes, followed by radiolarites and siliceous clays with intercalations of carbonates. Early Carnian Hallobia Beds within the Meliata facies zone and Late Carnian to Early Rhaetian Hallstatt Limestones clearly indicate a carbonate increase. Similar sediments like in the Hallstatt Limestone facies zone can be expected in the Meliata facies zone from this time on as well. These sediments are only preserved as breccia components within mass transported deposits. Slight differences in the sedimentary record of the

distal continental margin of the Eastern Alps/Western Carpathians and the Dinarides/Albanides and Hellenides also help for the integration of rocks to a specific paleogeographic environment. These are summarised in Gawlick et al. (2017a). The main contrasts are:

1. Intense volcanism and deposition of volcanic ashes is widespread in the Northern Calcareous Alps and the Western Carpathians at the time of the Neo-Tethys break-up (Gawlick et al., 2012a). Instead, the Dinarides and Southern Alps are only affected in several parts.
2. Within the Dinarides, radiolarites are the predominant sediments within the distal continental margin (Hallstatt and Meliata facies zone) in the Late Anisian to Late Ladinian (Kovács et al., 2011). In contrast, the Eastern Alps/Western Carpathians are affected only in the Meliata facies zone by radiolaritic sedimentation (Gawlick & Missoni, 2015).
3. Middle Carnian siliciclastics are missing in the various coloured Hallstatt Limestones of the Dinarides, indicating here a sedimentary gap in the north Halobia shales (Gawlick & Missoni, 2015; Sudar et al., 2015).
4. The Dinarides/Albanides/Hellenides are not affected by the Rhaetian – earliest Jurassic siliciclastic event, instead of the Eastern Alps/Western Carpathians (Krystyn, 2008).

Nevertheless, similarities of the oceanic sediments and the continental slope clearly correlate with the overall paleoenvironmental conditions within the Neo-Tethys Ocean.

With the onset of the Wetterstein platform in the Late Ladinian a transition to carbonate sedimentation is visible practically in all facies zones. A stop of the carbonate production by the "Mid-Carnian" event led to the deposition of siliciclastics. Shallow water carbonate production started again in the Late Carnian, followed by the formation of the Hauptdolomit/Dachstein Carbonate Platform evolution. Optimum climatic and geodynamic conditions supported the production of huge amounts of carbonate in the Norian and Rhaetian. In this time the outer shelf margin is characterised by various coloured hemipelagic limestones. Intercalations of shallow water turbidites appear in the reef near facies zone, where radiolarites and bedded limestones with chert nodules are dominant at the continental slope. A pelagic environment established in all facies belts after the drowning event at the Triassic/Jurassic boundary. Sedimentation is missing on the morphological hights and a lack of sufficient sediment supply also led to the drowning of the Hauptdolomit/Dachstein Carbonate Platform. Extreme condensed sedimentation caused the formation of ferrous crusts. The change from rifting to compression within the Neo-Tethys Ocean resulted in a dramatic change of the sedimentation conditions since the late Early to Middle Jurassic (Gawlick et al., 1999a), resulting in predominant siliceous sedimentation (Schlager & Schöllnberger, 1974). From this time on, the Austroalpine domine attained the lower plate position (Gawlick et al., 1999a). Trench like basins established in front of the propagating thrust belt of the overriding ophiolites. Within the Northern Calcareous Alps and the Inner Western Carpathians, the obducted ophiolite nappe stack is not preserved. Only blocks of the distal continental margin and the ocean floor within Late Jurassic – Early Cretaceous deep-water basins prove this stage of obduction. With the change of the tectonic regime the interpretations of the Neo-Tethys belt is therefore discussed controversially (Tollmann, 1985, 1987; Gawlick et al., 1999a; Faupl & Wagreich, 2000; Frank & Schlager, 2006; Schmid et al., 2008).

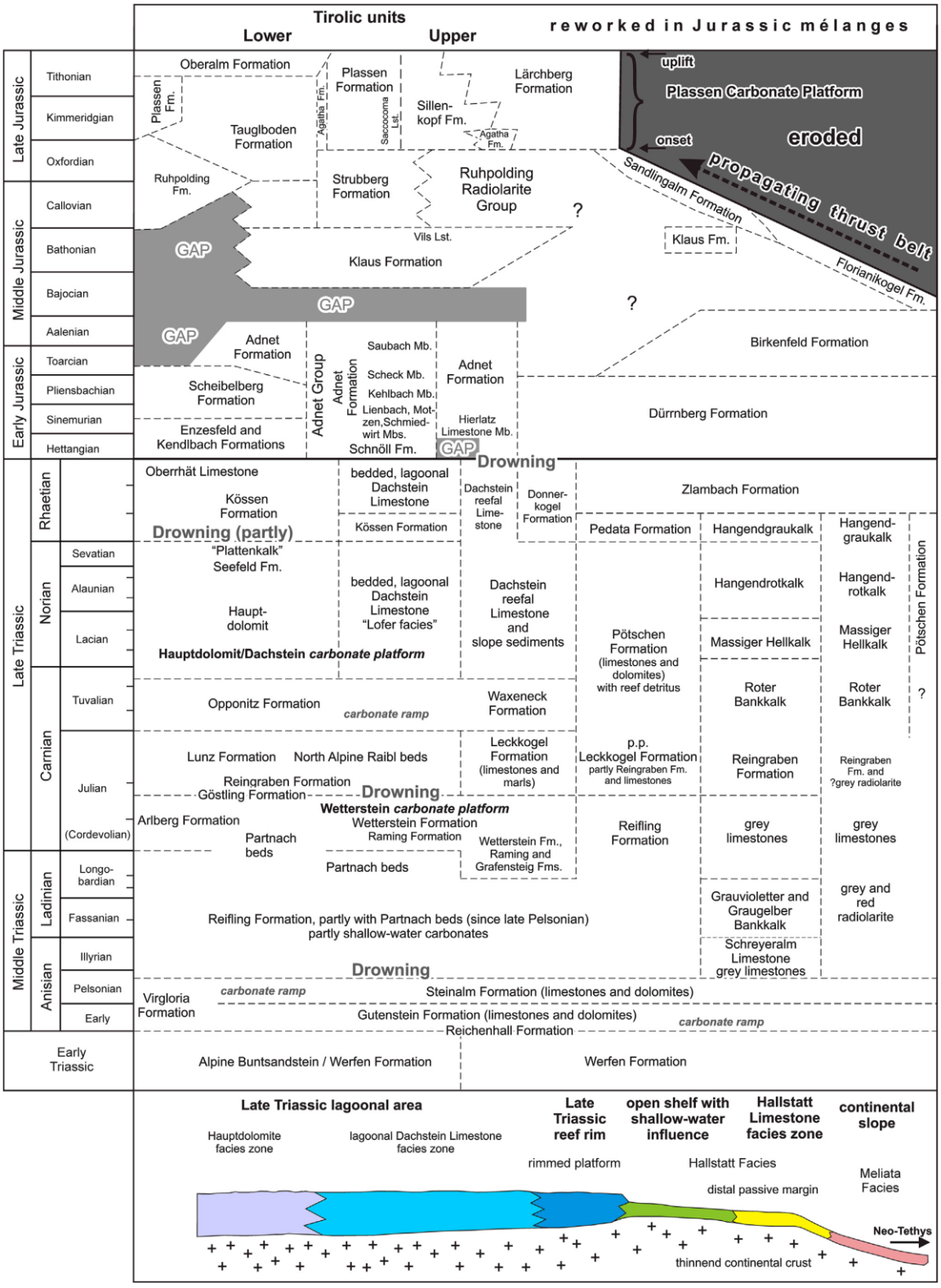

Figure 2: Stratigraphic table for the Triassic and Jurassic of the southern Northern Calcareous Alps, referred to the Middle to Late Triassic passive margin configuration after Tollmann (1985), Piller et al. (2004), Gawlick et al. (2009) and Missoni & Gawlick (2011a,b). For the color interpretation of the different facies belts see Figure 1.

2 Geological overview

2.1 Inner Western Carpathians

The Western Carpathian orogenic system form an E-W orientated mountain range, that represents the northern part of the European Alpides. The External Western Carpathians in the north, forms the Cenozoic accretionary complex of the overridden European foreland (also known as Flysch Belt). The southern part is instead built up by several thrust sheets, with a main tectonic movement in Jurassic to Cretaceous times (Gawlick & Missoni, 2019). They are further subdivided into the Central Western Carpathians (CWC) and Inner Western Carpathians (IWC) after Plašienka (2018). These three super units are separated by temporally active suture zones of extreme shortening, which may contain ophiolitic material (Plašienka et al., 1997).

The IWC, part of the Neo-Tethys Orogenic Belt (Alpine-Carpathian-Dinaric-Hellenic) can be subdivided in three tectonic subunits. From bottom to top, they are subdivided into the Meliata, Torna and Silica nappe, which are thrust over the Gemeric basement of the CWC (Plašienka, 2018) (see Figure 3).

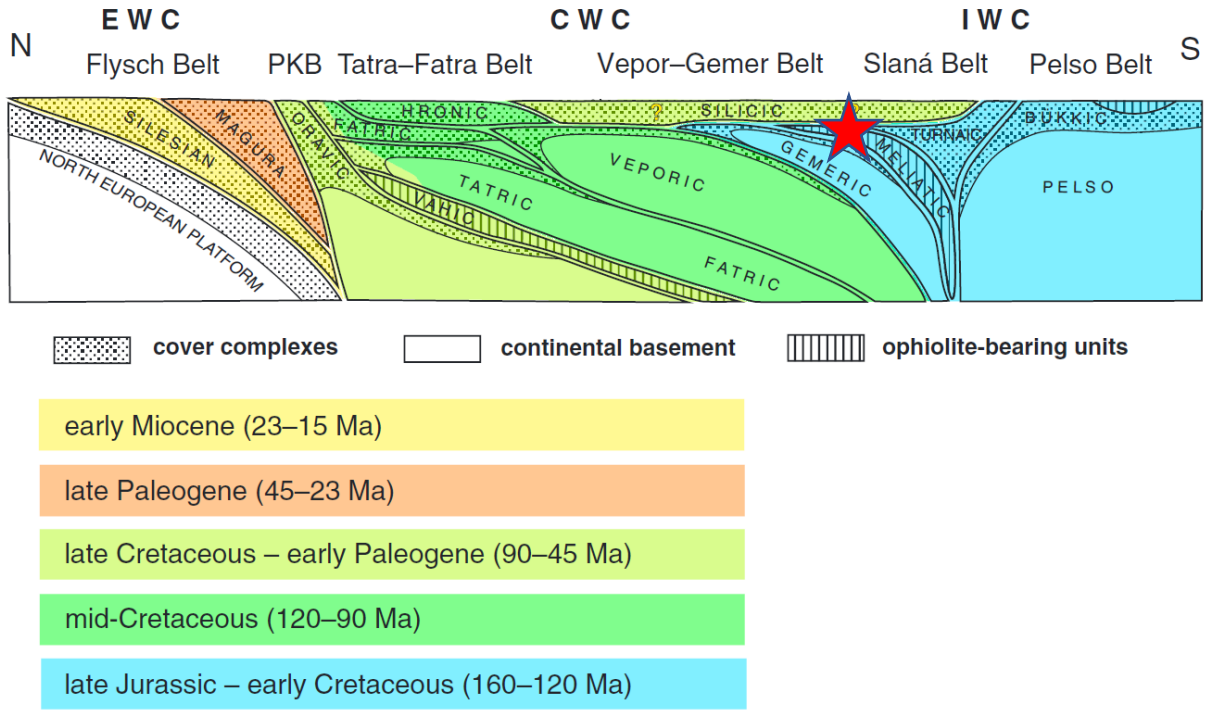

Figure 3: Schematic cross section of the Carpathian tectonic superunits after Plašienka (2018).The color denote the ages of the most important deformation and incorporation into the orogenic wedge. The investigated Meliata unit is marked in the profile with a red star.

In this study, we re-visited parts of the Meliata unit in the IWC (in sense of Plašienka, 2018), i.e. the well-known ophiolitic mélange in the Jaklovce area with special focus on the siliceous intercalations between the ophiolite blocks (Figure 4).

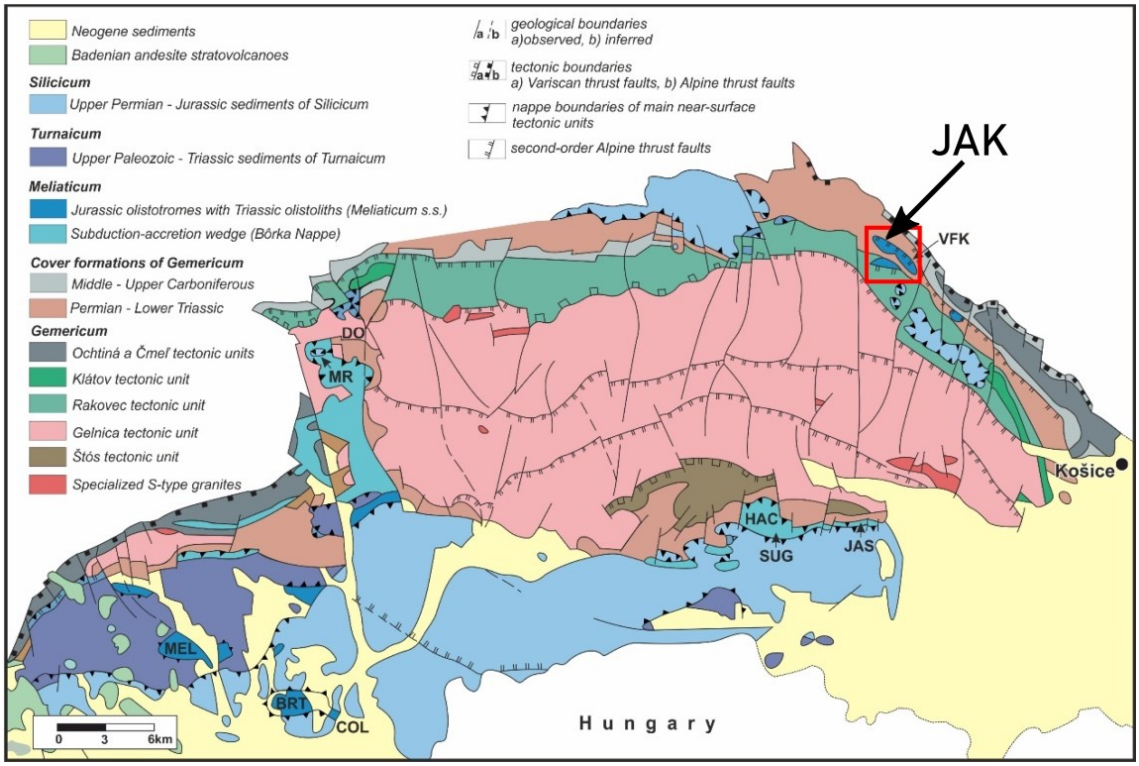

Figure 4: Tectonic map of the southern part of the IWC modified from Bezák et al. (2004) and Grecula et al. (2009). The red square shows the locality Jaklovce (JAK). Other locations of the Meliata type sections are: Dobšiná (DO), Veľký Folkmár (VFK), Brdárka (MR), Meliata (MEL), Bretka (BRT), Čoltovo (COL), Hačava (HAC), Šugov Valley (SUG); and Jasov (JAS).

The mélange blocks of Jaklovce were first investigated by Kamenický (1957) who mapped the basic rocks within the area. Based on Mock et al. (1998) and Putiš et al. (2019), these rocks are classified as N-MORB basalts, derived from the Neo-Tethys Ocean. On top of the known Middle Triassic (Kozur & Mock, 1985; Putiš, 2020) ophiolites, a relatively thick oceanic sedimentary sequence is preserved, which may reflect the early opening history of the Neo-Tethys Ocean (Meliata Ocean in other nomenclature: Kozur (1991), Mello et al. (1998), Ivan (2002)). Intercalations of reddish shales within massive volcanic layers are supposed to be Early Ladinian in age (Kozur & Mock, 1985). However, this age is not proven so far. Due to the relatively old age this block derived from a palaeogeographic position relatively near to the continental slope because the oceanic break-up of the Neo-Tethys started in Late Pelsonian times (Lein & Gawlick, 2008) and the oldest known oceanic crust is Illyrian (Goričan et al., 2005; Gawlick et al., 2008). Further, Putiš et al. (2019) confirmed the time of sedimentation by radiolarian dating from the Ladinian to the Late Carnian. A late Middle Jurassic matrix age of the mélange was still postulated by Kozur & Mock (1995), which is confirmed by Aubrecht et al. (2010).

U-Pb SIMS ages of 247 ± 4 Ma and 243 ± 4 Ma were determined from cherty shales, what shows a Middle Anisian age and xenocryst Zrn age of 266 ± 3 Ma from a basalt layer constrain roughly an Middle Anisian age (Putiš et al., 2019). Zrn Concordia ages of 342 ± 5, 359 ± 7, 488 ± 7, and 505 ± 13 Ma represent the underlaying Gemeric type Early Paleozoic basement complex (Putiš et al., 2019). The U–Pb SIMS metamorphic Rt age from metabasalts show an approximately 100 Ma age of a probable reburial and overheating event in late Early Cretaceous times (Putiš et al., 2019). Beside the age dating, the REE pattern and other immobile element ratios indicate an oceanic crust to back arc or marginal oceanic basin affinity of the basalts (Putiš et al., 2019). N-MORB or OIB basalts are most

likely. LREE depletion and HREE enrichment suggests a N-MORB to tholeiitic arc basalt (Putiš et al., 2019).

2.1.1 Jaklovce controversies

In older literature (Haas et al., 2011 with references therein) the differentiation of such mélanges in northern Hungary and in the Inner Dinarides of Serbia without consideration of their exact component spectrum, matrix age, microfacies and detailed sedimentological evolution also led to the existence of several independent oceans between microcontinents. All these mélanges should all differ from each other in composition and tectonic evolution (Dimitrijević et al., 2003).

The contribution of Triassic radiolarites to the ocean floor of the Meliata unit (Kozur, 1991; Mock et al., 1998) and the invention of a new ocean system ("Meliata ocean") by Kozur (1991) is therefore a result of lacking knowledge and disregarding the similarity of rocks. Therefore, Kovács et al. (2010, 2011) redefined the term Meliata regardless of the recent tectonic position or metamorphic overprint as the most distal Triassic-Jurassic facies belt.

The possibility of Middle Triassic radiolarite deposition on the Neo-Tethys open shelf setting (Goričan & Buser, 1989; Gawlick & Missoni, 2015 with references therein) and the association with intra-plate basalt (Pamic, 1984) gave cause to re-interpret the controversial term "Meliata" (e.g., Csontos, 2006; Froizheim et al., 2008; Kovács et al., 2010, 2011; Plašienka, 2018; Gawlick & Missoni, 2019). First mélange analysis of the Triassic and Jurassic Meliata facies zone are done by Mock et al. (1998), which are later expanded by new data from Aubrecht et al. (2010, 2012). Nevertheless, within the Meliata type area, the term Meliaticum still comprises several tectonic units e.g. Meliata s. str., Borka, Jaklovce (Plašienka, 2018). This subdivision is based on the imagination that all these units reflect different positions and metamorphose conditions within the overthrusting Nappe. Therefore, the Borka unit represents the lowermost position and the Jaklovce unit the uppermost position, with the Meliata unit s. str. in between. This also led to the thesis that these units are tectonic windows (Plašienka, 2018), based on the geological map of Slovacia (Mello et al., 1997).

Gawlick et al. (2017a) and Gawlick & Missoni (2019) reinterprets the Meliata type section and the corresponding Coltovo section as a sedimentary mélange with reworked material from the continental slope and the oceanic domain, deposited in trench like basins in front of the propagating nappe stack of obducing ophiolites. This is based on various analysis of metamorphic and non-metamorphic blocks within the non-metamorphosed matrix (Meliata unit: e.g., Kozur et al., 1996; Kozur & Mock, 1997; Mello et al., 1997; Dallmeyer et al., 2008; Plašienka, 2018). The Borka unit (Leško & Varga, 1980; Mello et al., 1998; Plašienka, 2018) which became metamorphosed under blueschist facies conditions (Mahel, 1986; Arkai et al., 2003) instead is interpreted as a tectonic mélange of an accretionary complex in Late Middle to Late Jurassic times (170/ 160–150 Ma: Maluski et al., 1993; Faryad & Henjes-Kunst, 1997; Dallmeyer et al., 2008). The Jaklovce unit includes the most distal mélange source and represents the characteristic oceanic or sedimentary-magmatic succession of the Meliaticum (Mock et al., 1998; Aubrecht et al., 2012; Putiš, 2020). This partly metamorphosed blocks of Triassic age (Dumitrică & Mello, 1982; Putiš et al., 2019; Putiš, 2020) within a Middle Jurassic, low-temperature anchimetamorphosed matrix (Mock et al., 1998; Aubrecht et al., 2012) are interpreted as a mega-olistolith (Kozur & Mock, 1985) which is deposited within ophiolite basins of the propagating nappe stack (Gawlick & Missoni, 2019; Putiš et al., 2019). Such similar volcanic rocks of the Raucherschober/Schafkogel within the Northern Calcareous Alps, many kilometers away from the type-locality Jaklovce give cause for a complete reinterpretation of the geological situation.

2.2 Northern Calcareous Alps

The Northern Calcareous Alps as a part of the Austroalpine fold and thrust belt represent a narrow mountain range, running from the Rhine valley to the Vienna basin, where the continuation to the Carpathians is covered by Tertiary sediments (Tollmann, 1963). Since decades, the tectonic subdivision and geologic evolution is a complicated and controversial topic. Now, two tectonic subdivisions of the Northern Calcareous Alps are in contrast. The classic model of Haug & Lugeon (1904) is accepted with some modifications (Nowak, 1911; Hahn, 1913; Spengler, 1919) by many. It describes the subdivision of the nappes from North to South into a Lower Bajuvavic, an Intermediate Tirolic and an Upper Juvavic nappe.

The fact that different tectonic nappes of the Northern Calcareous Alps show similar facies integrations and vice versa led to a palinspastic restoration for the time before Miocene lateral extrusion and nappe stacking. Therefore, a subdivision into facies belts (see Figure 5) representing the passive continental margin of the Neo-Tethys Ocean was introduced (Frisch & Gawlick, 2003; Gawlick et al., 2009a). This required a further subdivision of the three tectonic units of the Northern Calcareous Alps in comparison with their main tectonic movement and incorporation into the nappe stack. For a detailed description also see Frisch & Gawlick (2003), Gawlick et al. (2009), Missoni & Gawlick (2011b). Therefore, the Bajuvavic unit represents the proximal part of the passive continental margin and the Juvavic unit the distal part, with the Tirolic unit in between (Frisch & Gawlick, 2003).

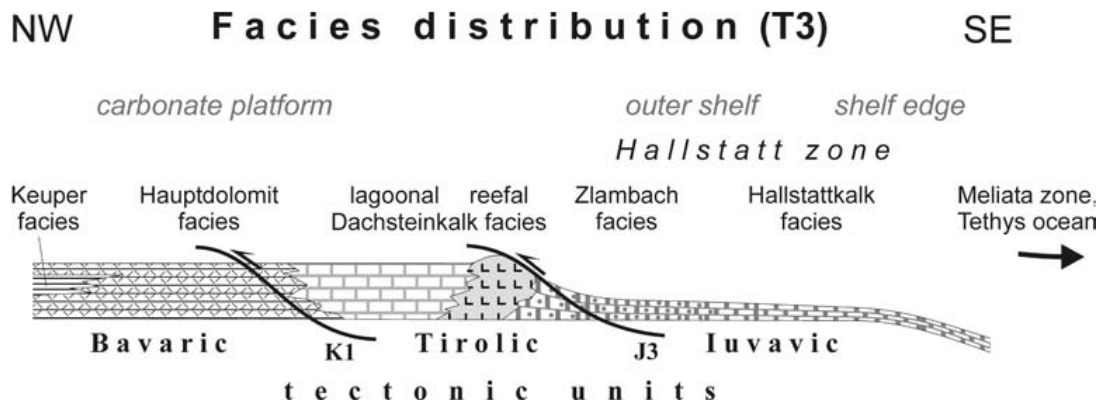

Figure 5: Schematic cross section of the passive Neo-Tethys margin form (Frisch & Gawlick, 2003), showing the facies distribution across the central Northern Calcareous Alps and the separation lines of the Juvavic, Tirolc and Bajuvavic nappe grouts in upper Triassic (T3), in Upper Jurassic (J3) and in Lower Cretaceous (K1) times.

2.2.1 Raucherschober/Schafkogel controversies

The Raucherschober and Schafkogel are located within the Northern Calcareous Alps at the boundary between upper Austria and Styria, east of Windeschgarsten (Figure 6). The exact integration to the regional tectonic framework of this area is controversially discussed in the past. According to Kober (1912), the Nordrandschuppe where the Raucherschober and Schafkogel belongs to is counted to the Lower Bajuvavic nappe and forms the NNE-SSW striking fault belt of Windischgarsten. Its composition derives from several Triassic rocks embedded in upper Cretaceous flysch like sediments (Plöchinger & Prey, 1968). These folded and tectonised blocks represent the north facing thrust horizon of the underlying nappes, dragged along the Haller Mauer and Gesäuseberge (Kraus, 1944).

In contrast, the Haller Mauer and Gesäuseberge are counted to the tirolic Warscheneck nappe by Tollmann (1962), which overthrusts the Lunz-Reichraminger nappe in northward direction. This affiliation of the Haller Mauer to the tirolic nappe is proven by Gawlick et al. (1994).

Based on the occurrence of Haselgebirge within the fault zone a juvavic position of the Nordrandschuppe, that is thrust over the tirolic Warscheneck nappe (Spengler, 1959) is rejected by Tollmann (1962) and Plöchinger & Prey (1968). Since then, no further integration of the Raucherschober and Schafkogel into the regional tectonic framework has been postulated.

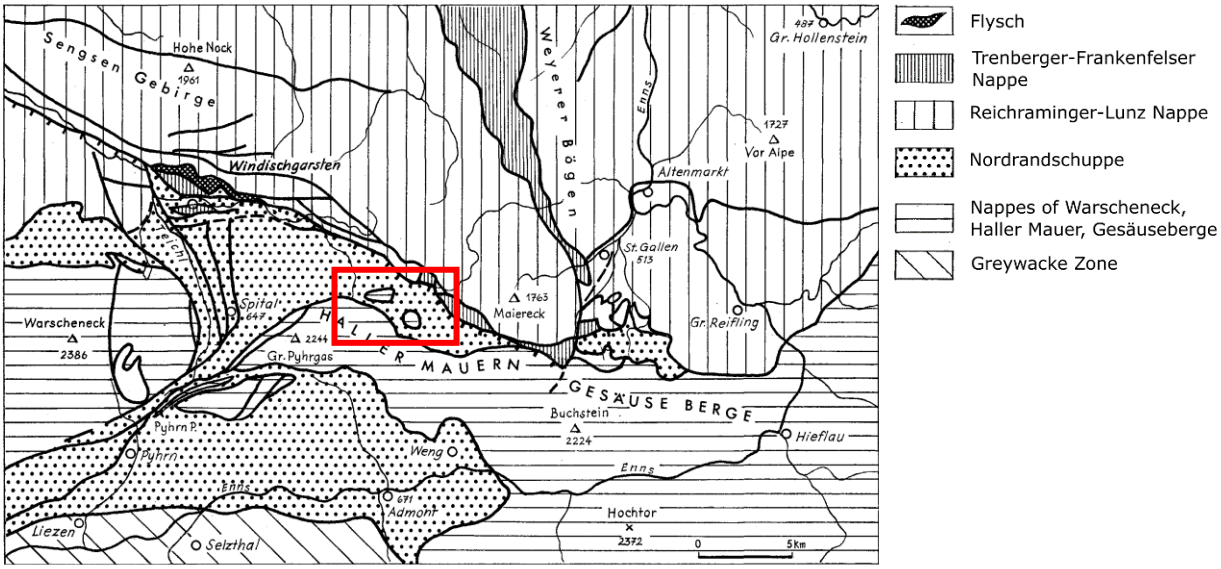

Figure 6: Geological map of the Windischgarstener window by Plöchinger & Prey (1968). The red square shows the location of the Schafkogel and Raucherschober within the Nordrandschuppe.

3 Sampling/Methods

Rock samples of two different mélanges from Jaklovce and the Raucherschober/Schafkogel were collected. In addition, the overlaying carbonates at the Raucherschober/Schafkogel are also sampled. For the record of the investigated mélange block at the railway near the Calwin company in Jaklovce (see Figure 7) and the close surrounding, 20 selected samples were collected and studied in detail. These are labelled with SD and a corresponding number. Six samples of volcanic ash are crushed to powder and analysed by X-ray diffractometry (XRD). Thin sections of these rocks are also studied in detail under the microscope. Within the area of the Raucherschober and Schafkogel, 100 samples of different rocks are analysed in this thesis. The sampling positions are shown in Figure 15. 88 of the 100 samples are labelled with R and numbered consecutively which were taken before this study began. The other 12 are labelled with LA and the corresponding number. The microfacies of the different limestones, as well as component analysis of sandstones and basaltic rocks are studied in detail by microscopical operations. For detailed element distributions of the basaltic rocks, several ICP-MS measurements are provided by the analytical testing and development services Actlabs (Table 1). Radiolarian bearing rocks are dissolved by diluted (3%) hydrofluoric acid and further detected by Scanning Electron Microscope. Conodont bearing samples are processed in diluted acidic acid.

4 Results

4.1 Jaklovce

Remnants of the distal passive continental margin and the ocean floor of the Neo-Tethys Ocean are incorporated in the Jaklovce mélange of the Inner Western Carpathians. In this study, one of these blocks is investigated, which is located north of Jaklovce village (Slovakia) near the Calvin company (Figure 7).

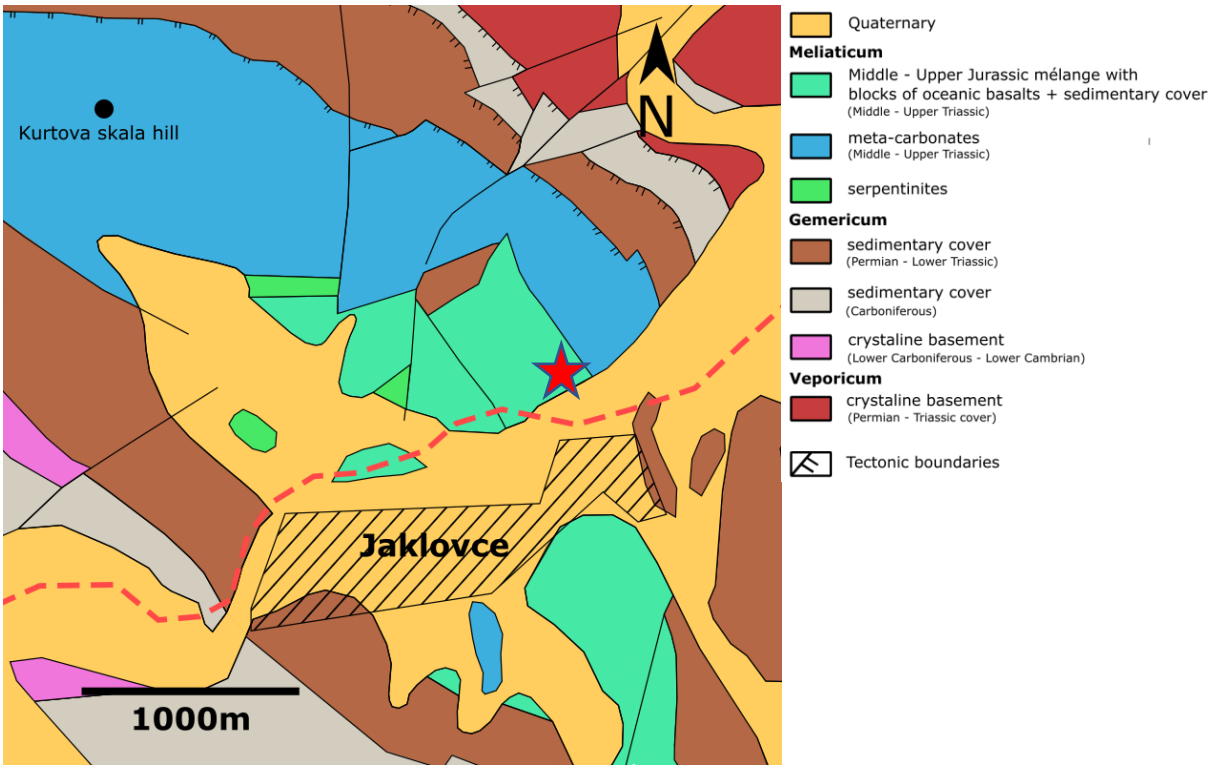

Figure 7: Simplified geological map of the Jaklovce area after Grecula et al. (2009). The sampled profile is marked with a star. The railway is shown by the red dashed line and the town is overdrawn with black parallel lines.

4.1.1 Sedimentary succession

The investigated Profile at the railway, consisting mainly of cherty shales and radiolarites, reaching a thickness of about 8m and dipping with a steep angle to the South (Figure 8).

Figure 8: The picture shows parts of the investigated sedimentary succession.

As the sedimentary cover of the ocean floor, the profile (Figure 9a) starts with an approximately one-meter-thick volcanic ash layer, which is cut by a fault (sample SD10). Feldspar, amphibole and low amounts of pyroxene are detected by XRD measurements and classify the sample beside the other minerals of chlorite and small amounts of quarz as volcanic rock (Figure 11). Portions of grey and green silicified clays with massive chert layers turn into a half of meter reddish and silicified clay. Again, grey and coarse-grained volcanic ash appears and reaches up to 10 cm thickness (sample SD9).

After, the succession turns into an approximately four-meter-thick part mainly consisting of red, silicified clays and radiolarites (sample SD4-2, SD12, SD11, SD4-1, SD6) with intercalations of greenish and grey, silicified volcanoclastics (sample SD8, SD12, SD13). Little amount of carbonate can be recognised in some beds in between. XRD measurements of the ashes show complete recrystallisation to quarz and chlorite (Figure 12). Low amounts of muscovite are also present. The presence of *Muelleritortidae* (Kozur 1988) in sample SD12 suggests a radiolarian age range from Longobardian to Cordovolian (Kozur & Moster 1996), which picture can be seen in Figure 9b.

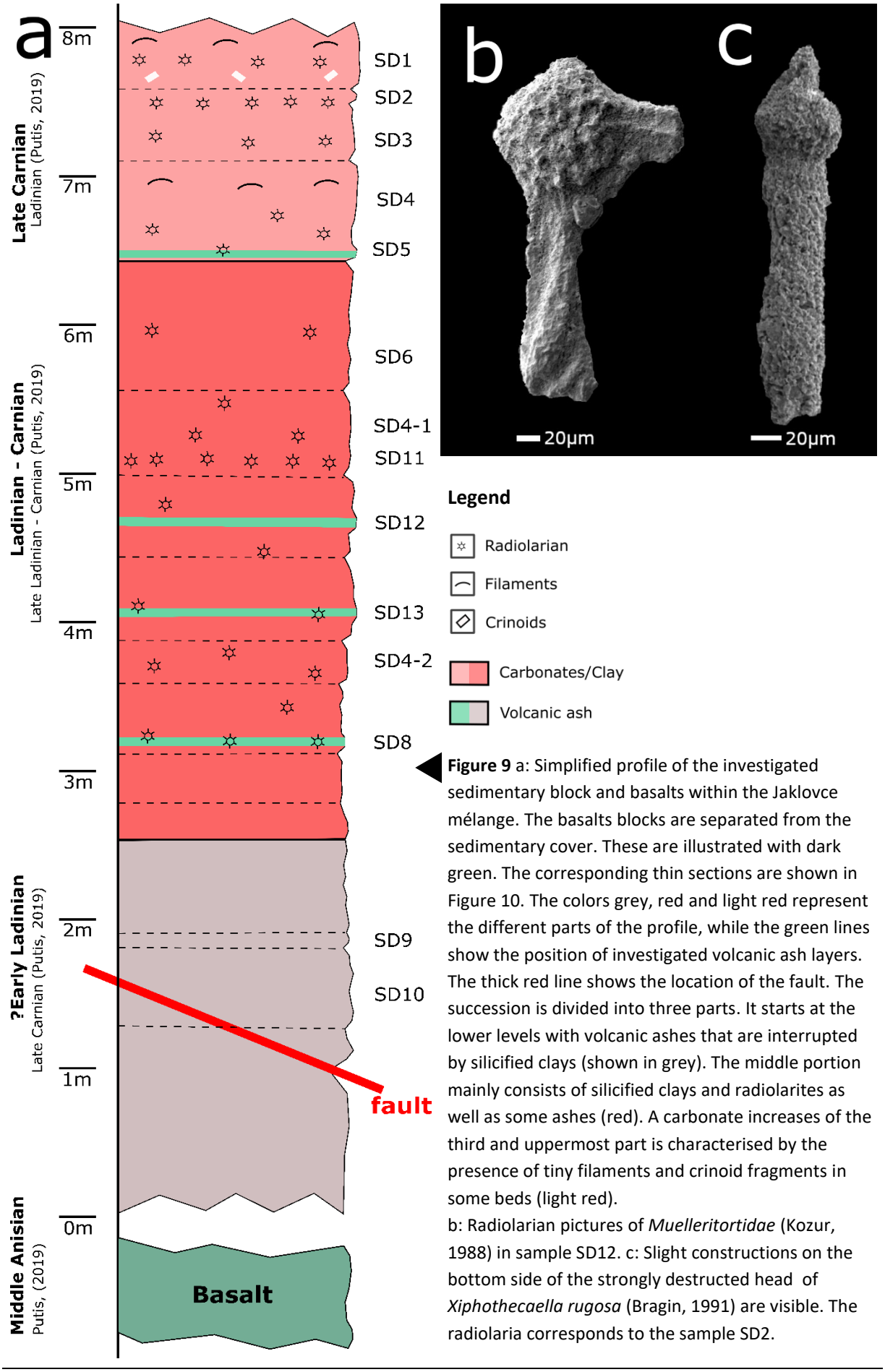

Figure 9 a: Simplified profile of the investigated sedimentary block and basalts within the Jaklovce mélange. The basalts blocks are separated from the sedimentary cover. These are illustrated with dark green. The corresponding thin sections are shown in Figure 10. The colors grey, red and light red represent the different parts of the profile, while the green lines show the position of investigated volcanic ash layers. The thick red line shows the location of the fault. The succession is divided into three parts. It starts at the lower levels with volcanic ashes that are interrupted by silicified clays (shown in grey). The middle portion mainly consists of silicified clays and radiolarites as well as some ashes (red). A carbonate increases of the third and uppermost part is characterised by the presence of tiny filaments and crinoid fragments in some beds (light red).
b: Radiolarian pictures of *Muelleritortidae* (Kozur, 1988) in sample SD12. c: Slight constructions on the bottom side of the strongly destructed head of *Xiphothecaella rugosa* (Bragin, 1991) are visible. The radiolaria corresponds to the sample SD2.

A change to more carbonate rich portions is visible in the uppermost part of the profile. Tiny filaments and crinoid fragments are present in some beds. The occurrence of *Xiphothecaella rugosa* (Bragin, 1991) within the sample SD2 not only determines an uppermost Carnian to upper Norian (Tekin, 1999) age, but it also defines the orientation of the profile within the mélange, from W – E to the hanging wall (see Figure 9c, and Figure 10).

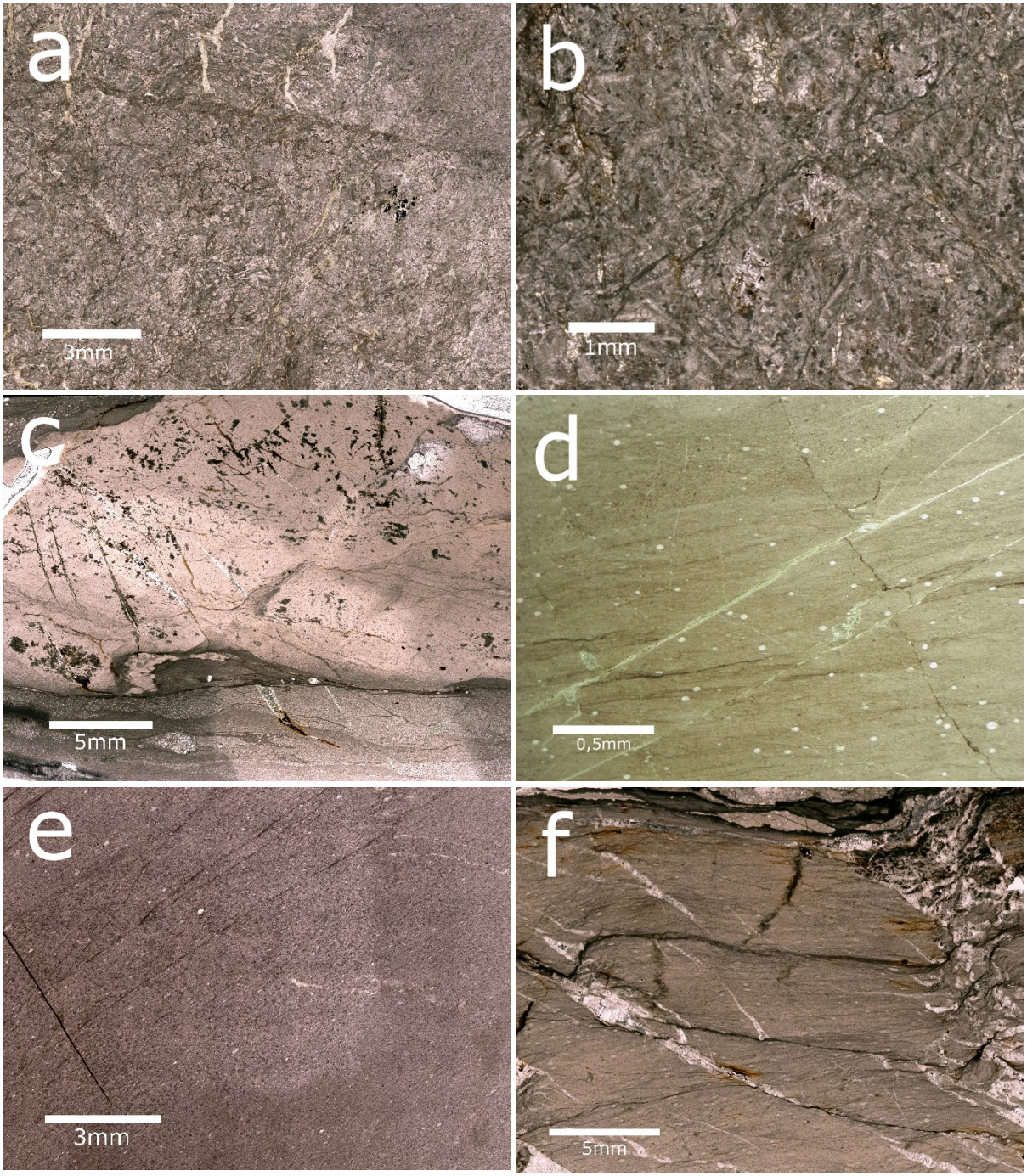

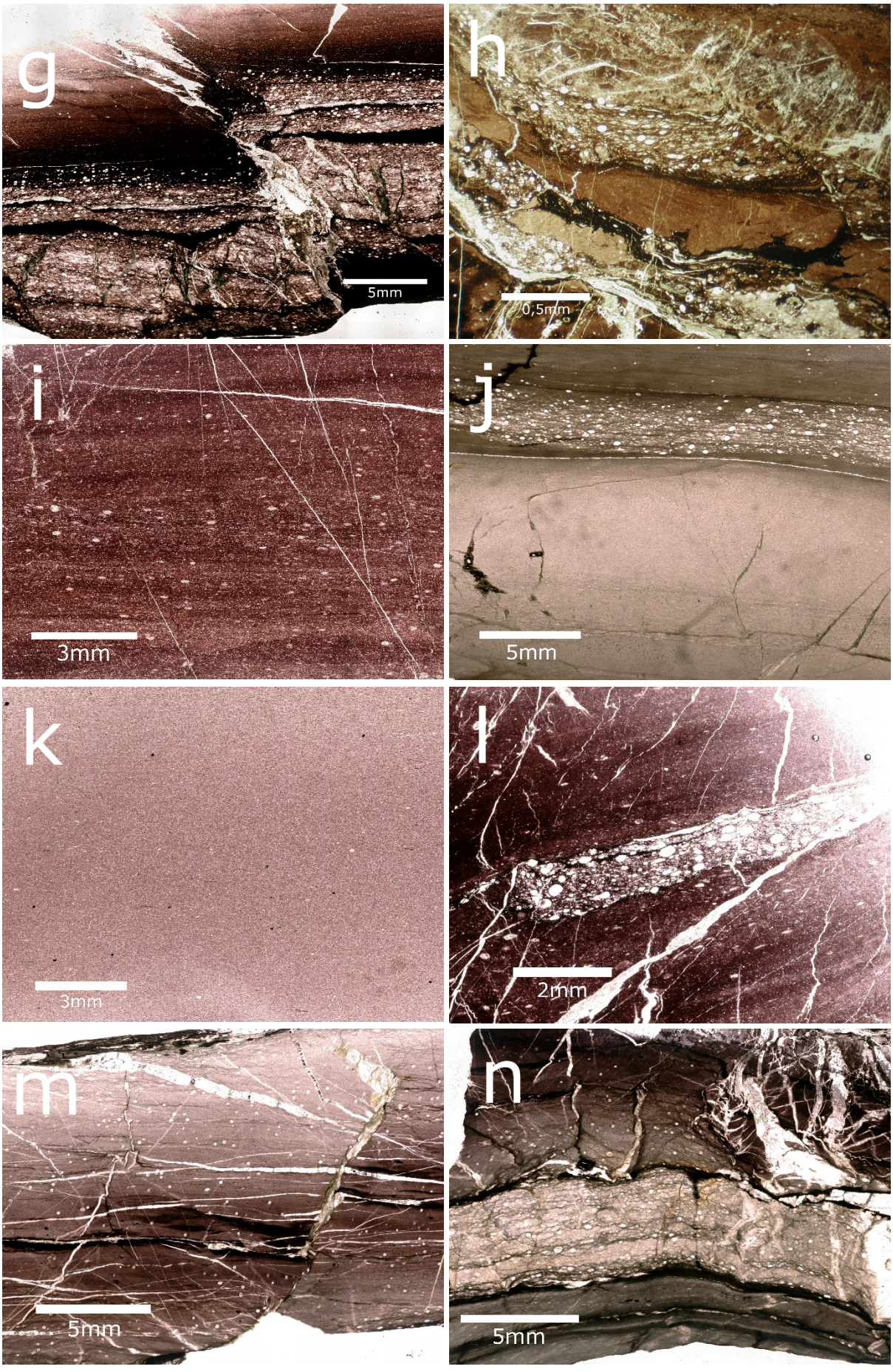
g
5mm
h
0,5mm
i
3mm
j
5mm
k
3mm
l
2mm
m
5mm
n
5mm

Figure 10: Samples of the investigated sedimentary succession at the railway. a: Grey and coarse volcanic ash (sample SD10). b: Grey and coarse-grained volcanic ash with a granoblastic texture. Small plagioclase crystals lay within a glassy matrix (sample SD9). c: Dark grey volcanic ash layers with radiolarian turbidites in between. The light portion is completely silicified (sample SD8). d: Silicified clay with some radiolarians in between (sample SD4-2). e: Dark and coarse-grained ash layer (sample SD13). f: Silicified volcanic ash with radiolarians of the species *Muelleritortidae* (Kozur, 1988) (sample SD12). g: Radiolarian turbidite shows synsedimentary thrusting. The matrix consists of red clay (sample SD11). h: Radiolarian turbidites within a red, clayey matrix (sample SD4-1). i: Red clay with some recrystallised radiolarians in between. The matrix is slightly carbonatic (sample SD6). j: Greenish and silicified ash with radiolarian turbidite on top (sample SD5). k: Reddish and marly clay (sample SD4). l: Red clay with radiolarian turbidite (sample SD3). m: Red ocean floor radiolarite shows dark condensed clay layers in between. The radiolarian species *Xiphothecaella rugosa* (Bragin, 1991) could be identified (sample SD2). n: The sample SD1 shows a sequence of dark, grey carbonates at the bottom, followed by greenish and silicified radiolarian turbidites and red clays with tiny radiolarians at the top.

All volcanoclastic layers of the middle part show complete recrystallisation to quarz and chlorite (Figure 12). Only sample SD8 contains little feldspar to classify the rock beside the typical greenish colour as volcanic.

In contrast, the lower part of the investigated profile shows a variety of minerals (Figure 11). Feldspar gets more abundant and actinolite and hornblende are the dominant amphibole minerals. This determines the rocks beside the granoblastic texture and the appearance of plagioclase within a glassy matrix (sample SD10, SD9) as volcanic derived. Pyroxenes are in small amounts detected as well.

Jurassic radiolarians within fractures give evidence for the mélange matrix. Investigations by Aubrecht et al. (2010) and Kozur & Mock (1995) revealed a late Middle Jurassic matrix age.

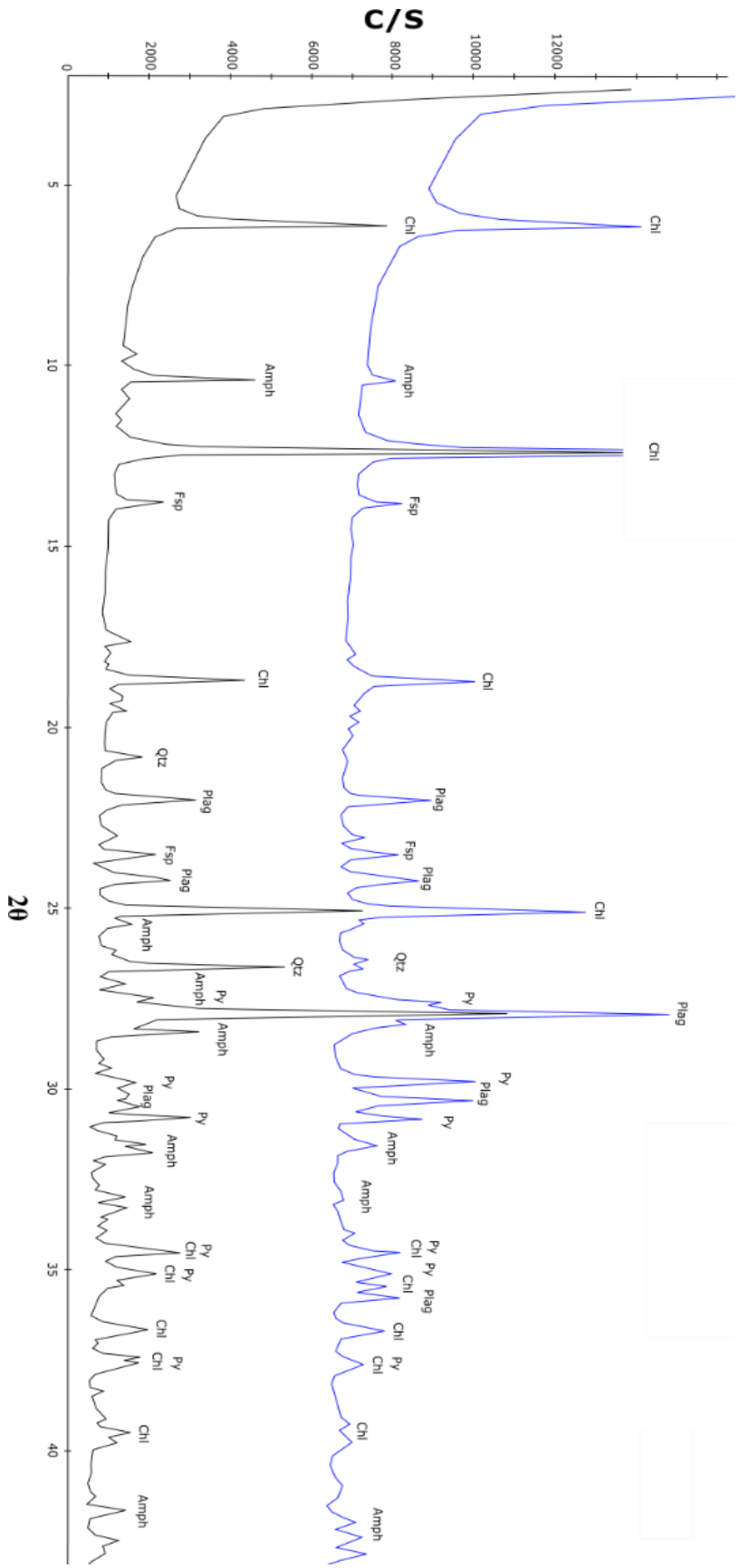

Figure 11: The Diffractogram of volcanic ash within the lower part of the Jaklovce profile. The black line corresponds to the sample SD9 and the blue line to the sample SD10. The Minerals are marked with Chl (chlorite), Qtz (quarz), feldspars are devided into Fsp (unspecific) and Plag for plagioclase, Py (pyroxene) and Amph (amphibole).

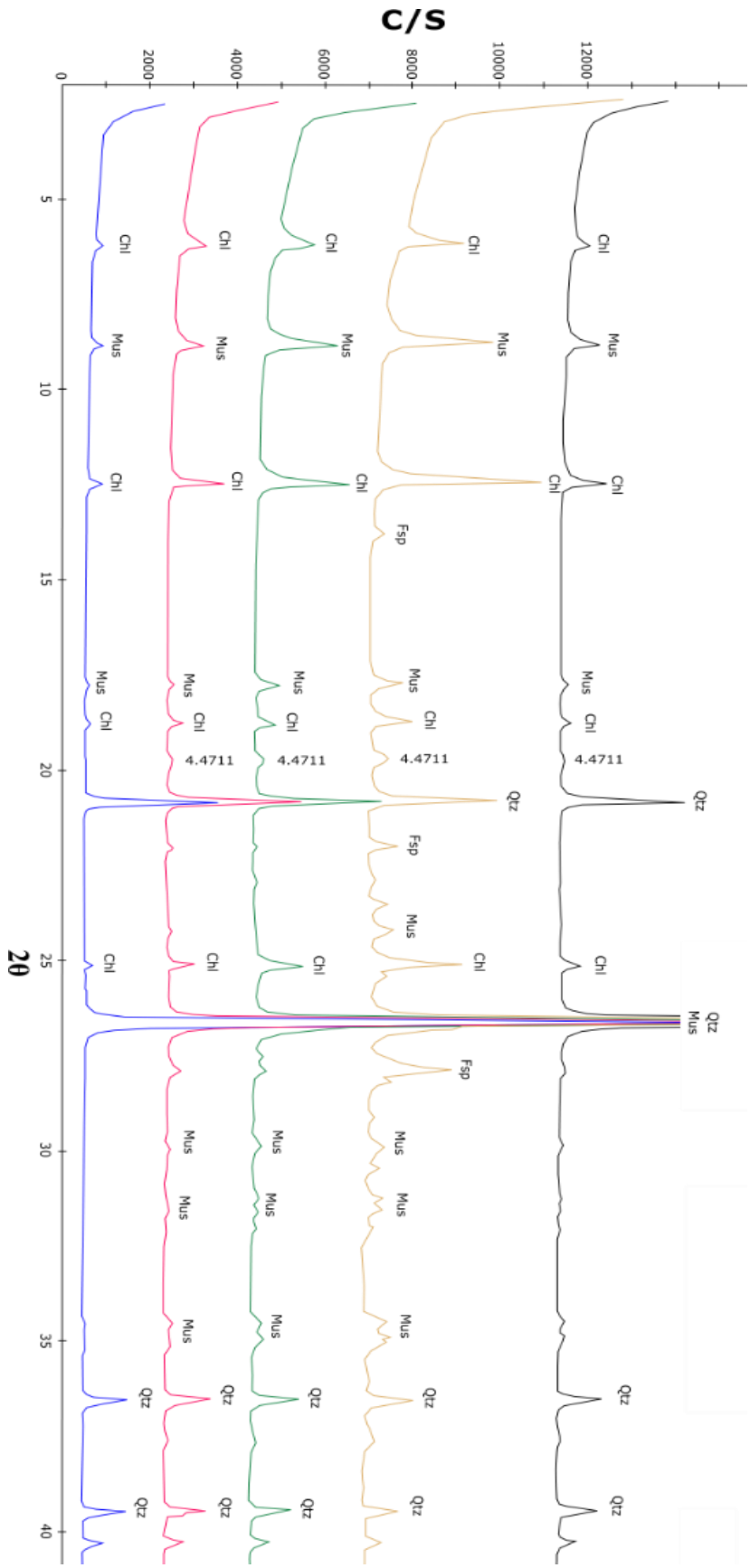

Figure 12: Diffractogram of volcanic ashes within the middle and upper part of the Jaklovce profile. The blue line corresponds to the sample SD1, the red line to the sample SD5, the green line to the sample SD7, the yellow line to the sample SD8 and the black line to the sample SD12. The minerals are marked with Chl (Chlorite), Mus (muscovite), Qtz (quarz) and Fsp (feldspar).

4.1.2 Surrounding

By following the railway from the Calwin company to the West, several metabasalt blocks, which are studied in detail by Putiš et al. (2019) are present. These pillow basalts often contain radiolarites and red silicified clays between the pillow structures that clearly indicate the contact of the basalt and the overlaying sedimentary succession (see Figure 13).

Figure 13: Overview pictures from the metabalsats. a: Metabasalt block with pillow structures are marked with the red – dashed line. The block is cut by a fault. b: Silicified radiolarite within the cavities of the pillow basalt (sample SD4-3).

Even if no radiolarians could be extracted from the complete recrystallised radiolarite (sample SD4-3) within the pillow basalt, the transition from the basalt to the sedimentary cover is studied in detail (Figure 14). In the sedimentary cover a metamorphic overprint appears within veinlets and the adjacent surrounding, building a network of newly formed chlorite, actinolite, epidote, feldspar, calcite and quarz. A gradual change from calcite richer portions at the contact of the metabasalt to quarz dominant veinlets within the overlaying sediment can be recognised. Magnetite is also common within the silicified sediment above the metabasalt which shows intergrowth with pyrite.

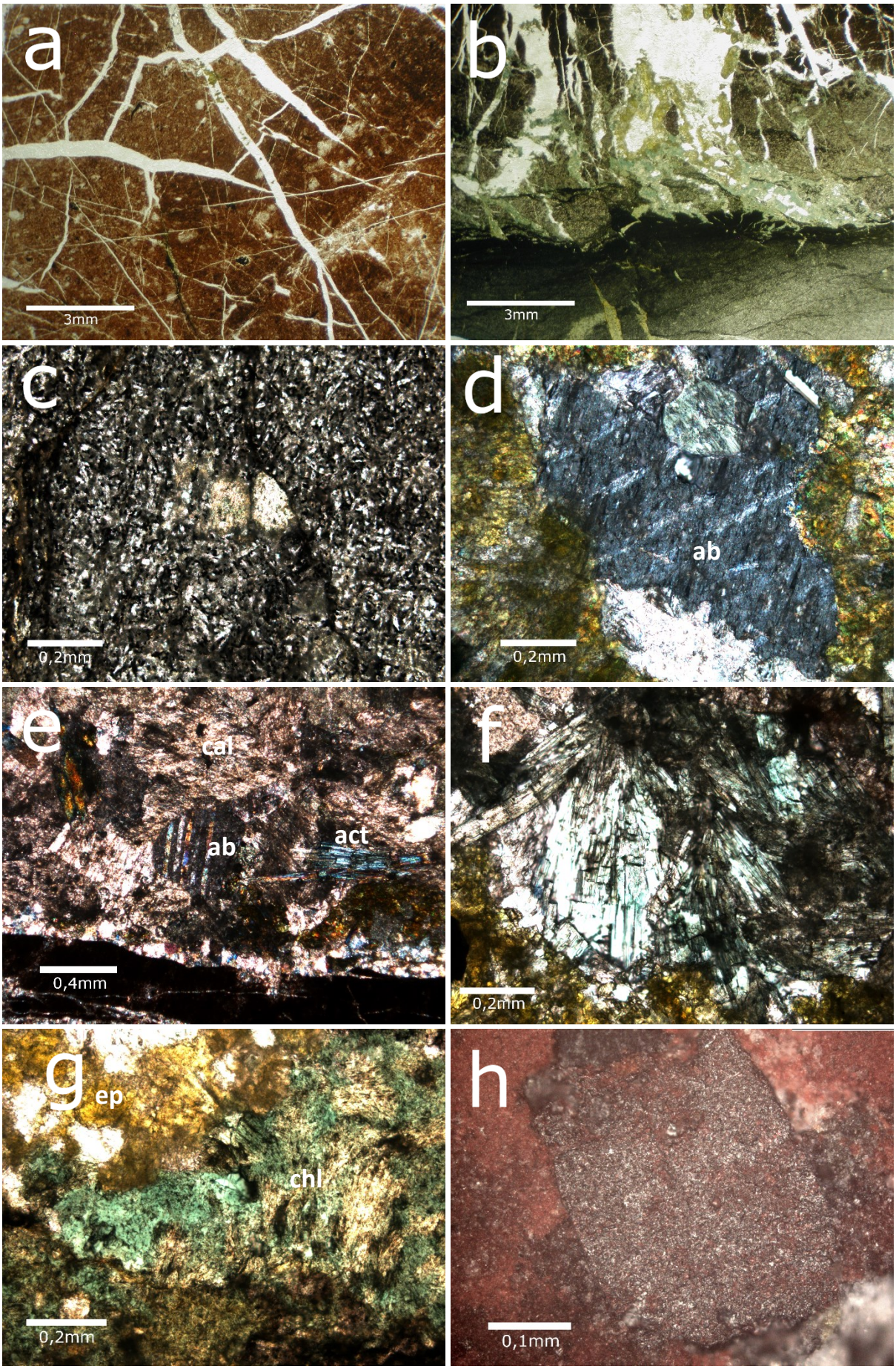
a
3mm
b
3mm
c
0,2mm
d
ab
0,2mm
e
cal
ab
act
0,4mm
f
0,2mm
g
ep
chl
0,2mm
h
0,1mm

Figure 14: Thin section pictures of the metabasalt at the contact to the overlaying sediments. a: Silicified radiolarite within a pillow cavity. All radiolarians show complete recrystallisation (sample SD4-3). b: Transition from the metabasalt at the bottom to the sedimentary cover at the top. A network of veinlets caused hydrothermal alteration and crystallisation of chlorite, actinolite, epidote and even feldspar (sample SD4-4). c: The volcanoclastic texture of the metababasalt is clearly visible. Plagioclase crystals lay within a dark-glassy matrix. Chloritisation is visible by the greenish color (sample SD4-4). d: Under polarized light albite (ab) shows typical twinning. The crystal is surrounded by epidote - (sample SD4-4). e: The contact of the metabasalt to the overlaying sediment shows complete recrystallisation. Albite (ab) and actinolite (act) crystals are surrounded by calcite (cal). Actinolitet shows blue interference colores - (sample SD4). f: Actinolite crystals show little pleochroism of light greenish colors. Interference colors from green to blue are typical. Sometimes diamond shaped cross sections are visible (sample SD4-4). g: Chlorite (chl) shows bright green and yellow interference colors. Epidote (ep) instead shows a typical off-colored yellow - brown (sample SD4-4). h: Crystals of magnetite, intergrown by pyrite within the sedimentary cover above the basalt (sample SD4-4).

4.2 Schafkogel/Raucherschober

In the Northern Calcareous Alps, north of the Mürzalpen nappe west of the Hengstpass a so far unknown Hallstatt mélange below the Late Jurassic Plassen Carbonate Platform contains beside several Hallstatt Limestone components also siliciclastics and volcanic rocks (see Figure 15). In this study biostratigraphic age dating of the matrix of the Hengstpass Hallstatt mélange and analyses of the different limestones and volcanic components are presented.

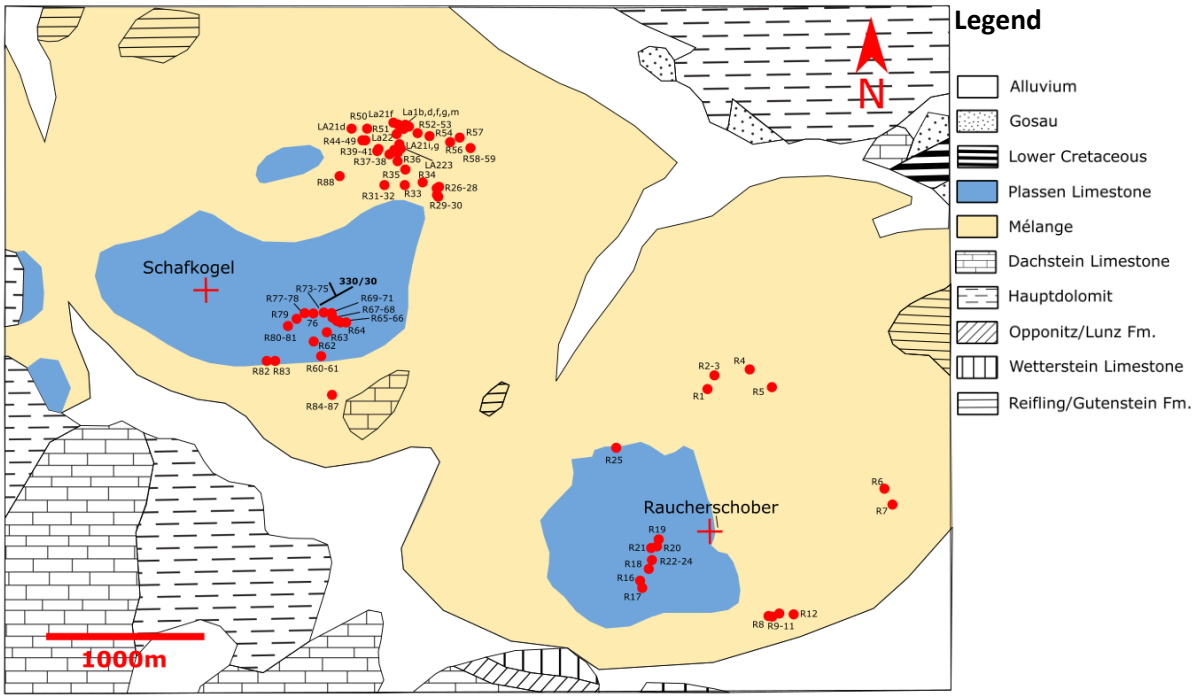

Figure 15 shows the modified geological map of the Raucherschober and Schafkogel after Plöchinger & Prey (1968). The Plassen Limestone is overdrawn with blue and the underlaying mélange is indicated with yellow. Because of limited investigation, the border of the mélange is speculative. The sampling points are shown as red dots.

Both, the Raucherschober, as well as the Schafkogel are topped by the Plassen Limestone that dip at a low angle to the NNW (Figure 15). These bioclastic wack - packstones of turbiditic origin show a basinal evolution, determined by siliciclastic input and the progradation of the adjacent Plassen Carbonate Platform sensu stricto. Below these carbonates, different blocks of various distribution

and age are present within a siliceous-argillaceous and soft matrix (see Figure 16). These mélange components all derive from the former continental margin of the Neo-Tethys Ocean.

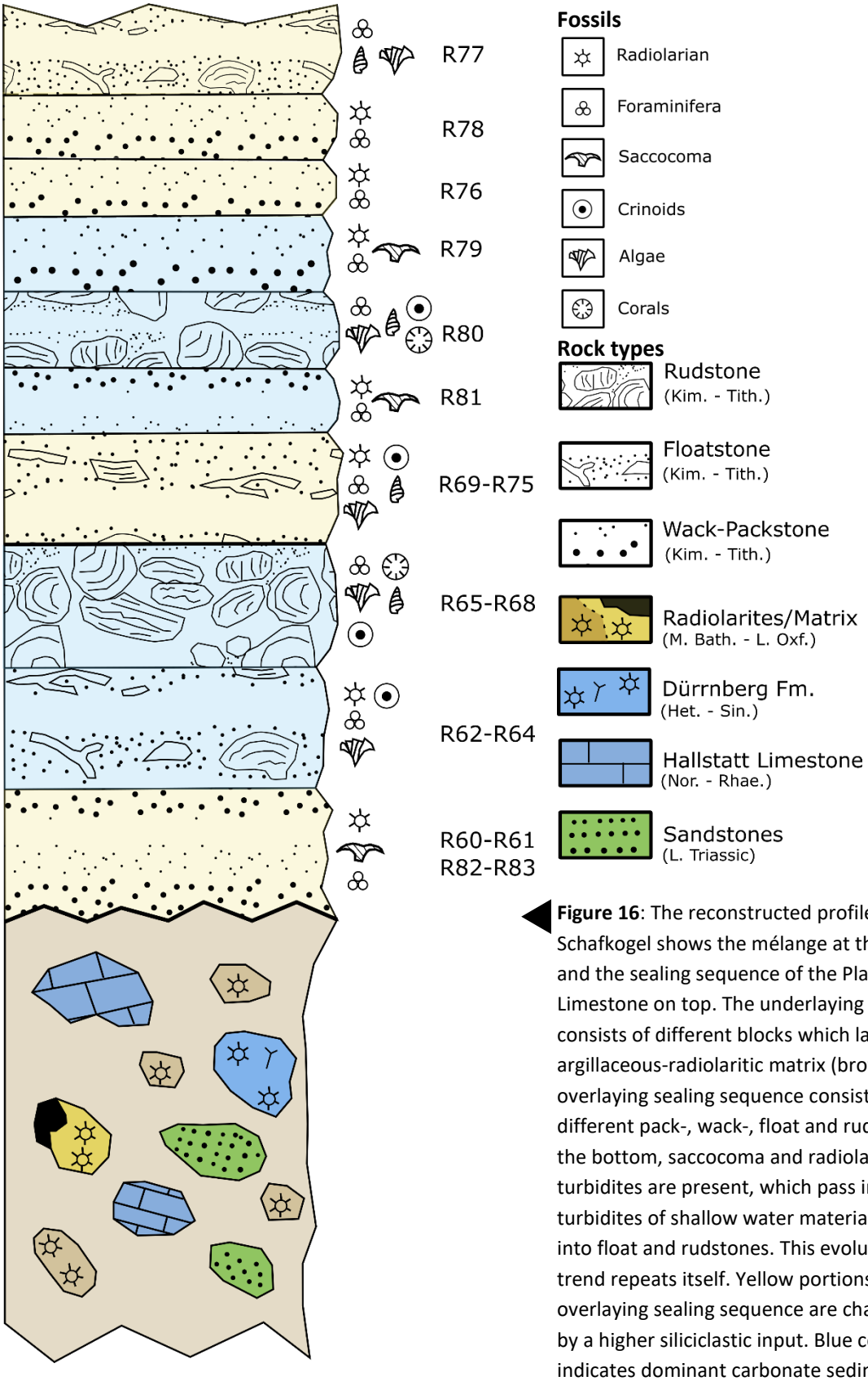

Figure 16: The reconstructed profile of the Schafkogel shows the mélange at the bottom and the sealing sequence of the Plassen Limestone on top. The underlaying mélange consists of different blocks which lay within an argillaceous-radiolaritic matrix (brown). The overlaying sealing sequence consists of different pack-, wack-, float and rudstones. At the bottom, saccocoma and radiolarian rich turbidites are present, which pass into turbidites of shallow water material and further into float and rudstones. This evolutionary trend repeats itself. Yellow portions of the overlaying sealing sequence are characterized by a higher siliciclastic input. Blue colorization indicates dominant carbonate sedimentation.

4.2.1 Components of the mélange

4.2.1.1 Siliciclastica

Two different types of sandstones which distinguish from each other by composition and grain size are recognised within the mélange (Figure 17). Fine grained and green sandstones with high quarz content can be assigned to a Jurassic age by the presence of small radiolarians (sample LA1g).

In addition, coarser grained and layered sandstones with a high amount of rock fragments are counted to be Werfener Beds (sample LA1m). These sandstones are the predominant siliciclastic rocks within the studied area. This is also confirmed by Plöchinger & Prey (1968), who mapped these areas in detail.

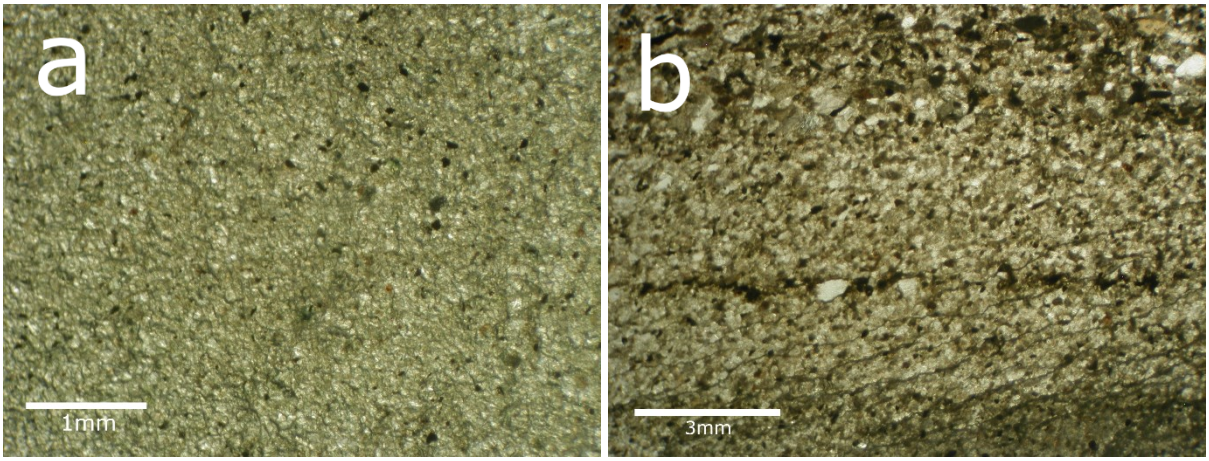

Figure 17: Sandstone samples within the Hengstpass Hallstatt mélange. a: Green and fine-grained sandstone with some tiny radiolarians (sample LA1g). b: Greenish and layered sandstone of the Werfener Beds mainly composed of quarz and rock fragments (sample LA1m).

4.2.1.2 Volcanic rock

Based on microscopical studies, no correlation to a basaltic rock is possible. Only large calcite crystals and some anorthite crystals which lay within or grow over the brown-glassy matrix can be distinguished (Figure 18).

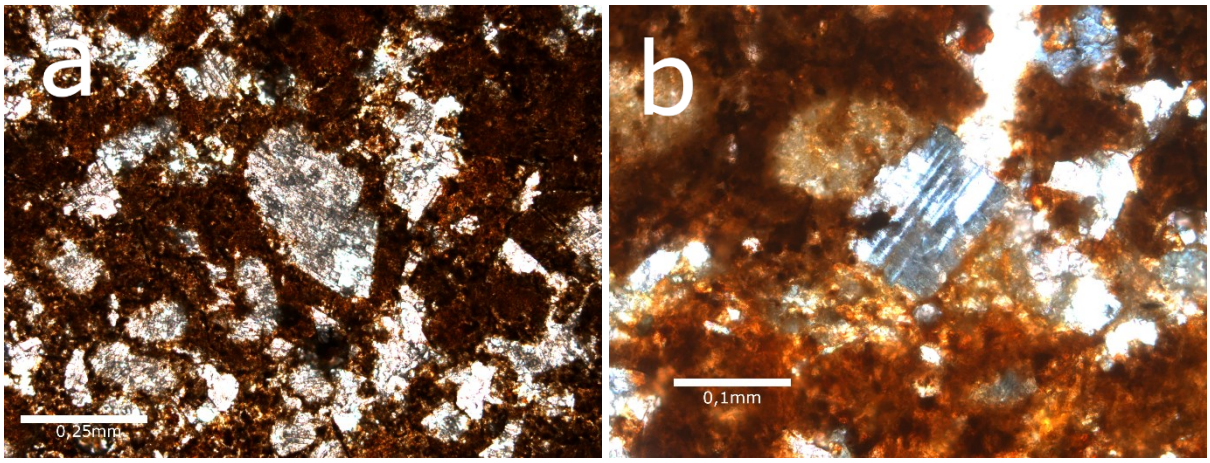

Figure 18: Thin section of the basalt. a: Nearly all primary minerals are replaced with calcite. The reddish - brown mass in between the calcite crystals represents the residual fragments of the primary rock (sample LA23). b: Secondary anorthite within a reddish - brownish glassy-matrix of the altered basalt. Under polarized light, the anorthite shows typical twinning (sample LA23).

Table 1 lists two major and trace element analysis of the sample LA23. Sample LA23a represents the unweathered, inner part and sample LA23b the more weathered, outer part of the sample. Therefore, nearly all elements of the LA23b sample are slightly enriched due to the removal of rock forming minerals. Compared with other basalts, a lack in SiO_2, Al_2O3 and Na_2O is clearly visible. Especially the extreme low SiO_2 value makes it impossible to classify the samples by using the standard diagrams for magmatic rocks. In addition, they have increased TiO_2, K_2O, MgO values and abnormal high CaO values.

analysed compound/element	sample LA23a	sample LA23b	analysis method
(%)			
SiO2	10.07	14.42	FUS-ICP
Al2O3	0.85	1.5	FUS-ICP
Fe2O3(T)	9.95	9.82	FUS-ICP
MnO	0.887	0.905	FUS-ICP
MgO	9.13	4.31	FUS-ICP
CaO	29.68	33.34	FUS-ICP
Na2O	0.39	0.62	FUS-ICP
K2O	0.05	0.13	FUS-ICP
TiO2	0.048	0.1	FUS-ICP
P2O5	0.02	0.04	FUS-ICP
LOI	37.38	33.84	FUS-ICP
Total	98.46	99.03	GRAV
(ppm)			
Sc	< 1	1	FUS-ICP
Be	< 1	< 1	FUS-ICP
V	12	17	FUS-ICP
Cr	< 20	< 20	FUS-ICP
Co	3	2	FUS-ICP
Ni	9	9	TD-ICP
Zn	16	14	TD-ICP

Cd	< 0.5	< 0.5	TD-ICP
S	0.023	0.01	TD-ICP
Cu	97	169	TD-ICP
Ag	< 0.3	< 0.3	TD-ICP
Pb	5	6	TD-ICP
Ga	2	2	TD-ICP
Ge	< 1	< 1	FUS-ICP
As	5	< 5	FUS-ICP
Rb	2	4	FUS-ICP
Sr	171	133	FUS-ICP
Y	22	24	FUS-ICP
Zr	44	93	FUS-ICP
Nb	1	2	FUS-ICP
Mo	< 2	< 2	FUS-ICP
In	< 0.2	0.2	FUS-ICP
Sn	< 1	< 1	FUS-ICP
Sb	< 0.5	< 0.5	FUS-ICP
Cs	< 0.5	< 0.5	FUS-ICP
Ba	24	83	FUS-ICP
La	7.6	14.8	FUS-ICP
Ce	20.5	34.7	FUS-ICP
Pr	2.66	4.11	FUS-ICP
Nd	12	17	FUS-ICP
Sm	3.5	4.3	FUS-ICP
Eu	0.84	1	FUS-ICP
Gd	3.8	4.5	FUS-ICP
Tb	0.7	0.8	FUS-ICP
Dy	3.9	4.3	FUS-ICP
Ho	0.7	0.9	FUS-ICP
Er	1.8	2.2	FUS-ICP
Tm	0.22	0.29	FUS-ICP
Yb	1.1	1.8	FUS-ICP
Lu	0.14	0.24	FUS-ICP
Hf	1.1	2.4	FUS-ICP
Ta	< 0.1	0.1	FUS-ICP
W	< 1	< 1	FUS-ICP
Tl	< 0.1	< 0.1	FUS-ICP
Bi	< 0.4	< 0.4	FUS-ICP
Th	1.9	3.9	FUS-ICP
U	0.6	1.1	FUS-ICP

Table 1: Major and trace elements from the whole-rock inductively coupled plasma mass spectrometry (ICP–MS) analyses. LOI = Loss on ignition.

According to the trace element configuration, the samples show calc-alkaline volcanic arc affinity (Figure 19, Figure 20, Figure 21). Incompatible elements like Rb, Ce, Ba, Pb, Th, Ga, U, as well as the LREE are significantly enriched. This represents low grade partial melting of oceanic crust and the fractionation of olivine and clinopyroxene, compared with fluid alteration of the dehydrated slab. Instead, relatively immobile elements like Nb, Ta, Zr, Hf, Y and HREE are clearly depleted. This is because of the abundance of the relatively immobile elements to more stable minerals like phlogopite or hornblende and the low affinity to the fluid phase, remaining in the subducting slab.

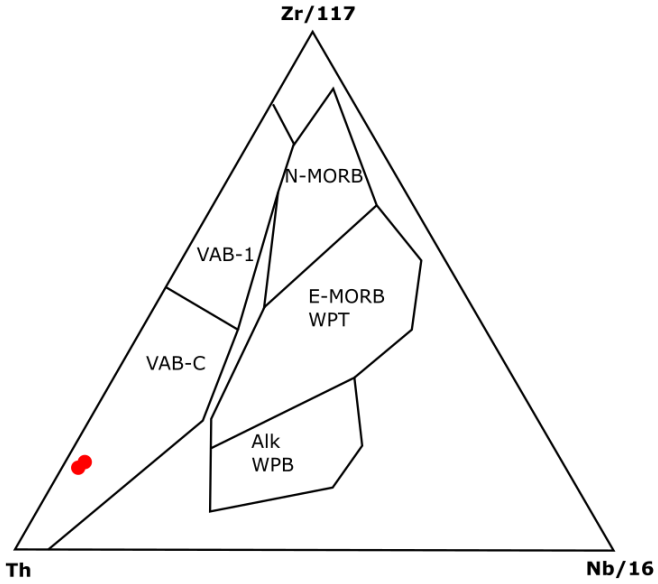

Figure 19: Zr/117–Th–Nb/16 discrimination diagram of Wood (1980) show the Schafkogel samples LA23a,b as red dots. Therefore, the rock can be classified to calc-alkaline volcanic arc basalts.
The fields within the triangle correspond to the alkaline within-plate basalts (Alk WPB), enriched mid-ocean ridge basalts (E-MORB), normal mid-ocean ridge basalts (N-MORB), calc-alkaline volcanic arc basalts (VAB-C), tholeiitic volcanic arc basalts (VAB-T) and within plate tholeiites (WPT).

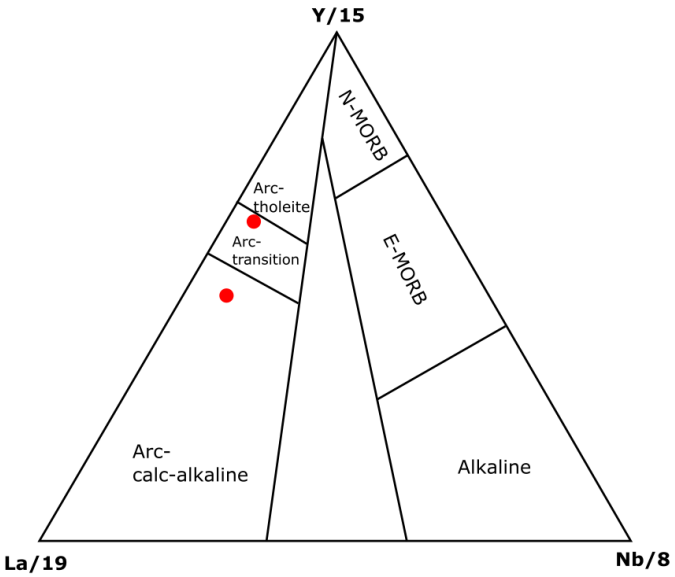

Figure 20: The diagram of Cabanis & Lecolle (1989) shows the geodynamic origin of the analyzed rocks as red dots (sample LA23a,b). A trend to arc magmatism of the LA23 samples is also visible here.

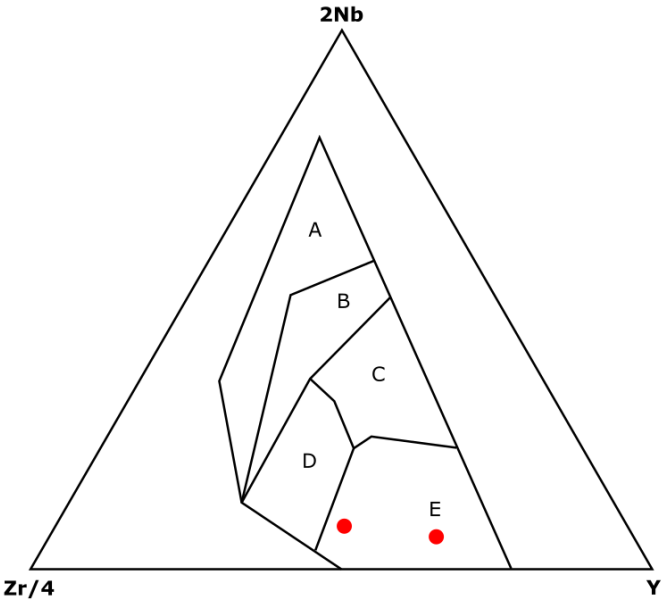

Figure 21: The geotectonic discrimination diagram Zr – Nb – Y of Meschede (1986) also plots the LA23a,b samples (red dots) within the volcanic arc basalt field.
The fields are: A—within plate basalts, B—within plate alkali basalts and within plate tholeiites; C—E-type MORB; D—within plate tholeiites and volcanic arc basalts; and E—N-type MORB and volcanic arc basalts.

The relative enrichment of the LREE compared to the HREE of the Schafkogel samples LA23a,b within the Chondrite normalised REE pattern is clearly visible (Figure 22). This also indicates a hydrous slab melting and the accompanied arc affinity.

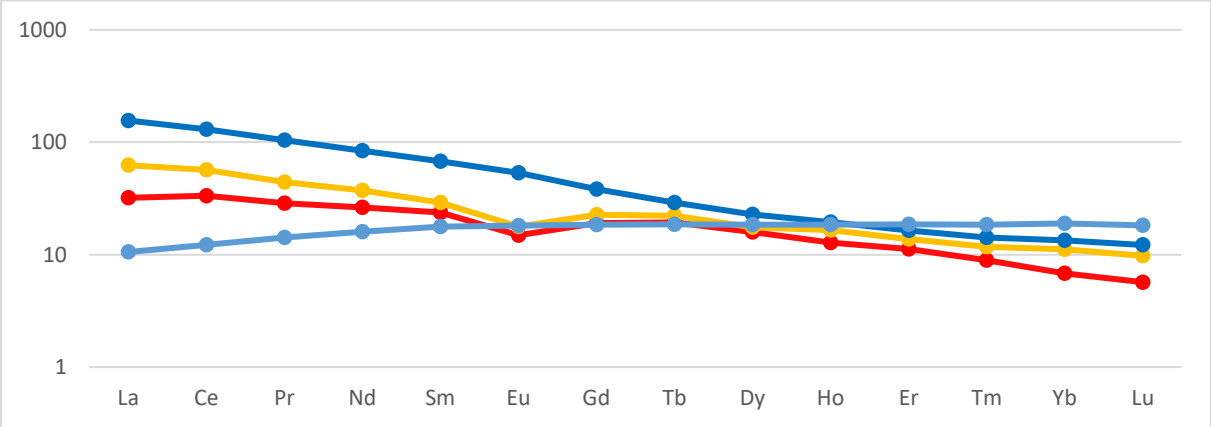

Figure 22: The Chondrite normalised REE pattern shows the analysed samples of the Schafkogel in red (sample LA23a) and orange (sample LA23b), in comparison to N-MORB basalt in light blue (Sun & McDonough, 1989) and OIB-basalt in dark blue (Sun & McDonough, 1989). Normalizing values are from Sun et al. (1979).

4.2.1.3 Hallstatt Limestone

The age of the Hallstatt Limestone components from the Hengstpass Hallstatt mélange dated by conodonts ranges from Norian to Rhaetian (Table 2). These red and grey bioclastic wack - packstones are studied in detail. Compared with the results of Mandl (1984) and Gawlick & Böhm (2000), a further subdivision into Hangendrotkalk and Hangendgraukalk is possible.

Sample name	Conodont species	Age
R48	*Hindeodella* sp. *Epigondolella* sp.	Norian
R57	*Norigondolella steinbergensis* (Mosher, 1968) *Epigondolella* sp.	Middle Norian
R49	*Norigondolella steinbergensis* (Mosher, 1968)	Alaunian - Sevatian
R53	*Norigondolella steinbergensis* (Mosher, 1968) *Misikella hernsteini* (Mostler, 1967) *Epigondolella bidentata* (Mosher, 1968) *Oncodella paucidentata* (Mostler, 1967)	Early Rhaetian
R54	*Oncodella paucidentata* (Mostler, 1967)	Early Rhaetian
R52	*Norigondolella steinbergensis* (Mosher, 1968) *Misikella hernsteini* (Mostler, 1967)	Rhaetian

Table 2: Conodont assemblages within the Hallstatt limestone. The age ranges from Norian to Rhaetian.

The abundant fossil framework of foraminifera, filaments and small shell fragments are accompanied by gastropods, echinoderms and ammonites within the Hangendrotkalk (Figure 23), representing a hemipelagic outer shelve margin setting.

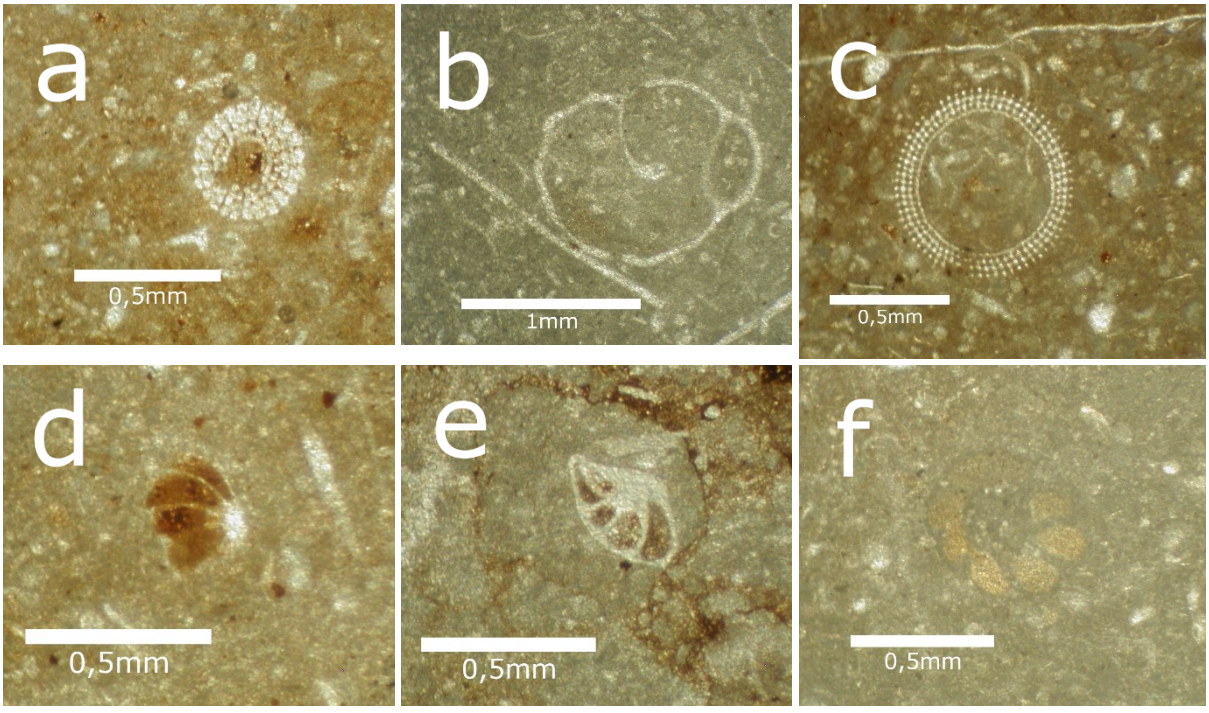

Figure 23: Microfacias table of the Hangendrotkalk shows a: Echinoderm (sample LA21f), b: Gastropod (sample R45), c: Radiolarian (sample R45), d: Ammonite fragment (sample R49), e: Calcite shell of a foraminifera (sample R47), f: Agglutinated foraminifera filled with oxidised micrite (sample R48).

Typical samples of the Hangendrotkalk are shown in Figure 24. Hemipelagic reddish – grey biomicritic limestones with filaments, foraminifera and shell fragments often show extensional features of the outer shelf margin (sample R45). The conodont assemblage of *Norigondolella steinbergensis* (Mosher, 1968) and *Epigondolella sp.* within the lumachelle of sample R57 suggests a Middle Norian age. Ostracods, echinoderms, foraminifera, as well as a coral colony can be found within the reddish - grey bioclastic packstone of intense stylolithisation (sample R49). The Alaunian - Sevathian conodont age is proven by the specie *Norigondolella steinbergensis* (Mosher, 1968). Condensed conditions of the hemipelagic limestones are often accompanied by hard ground formation (sample LA21f).

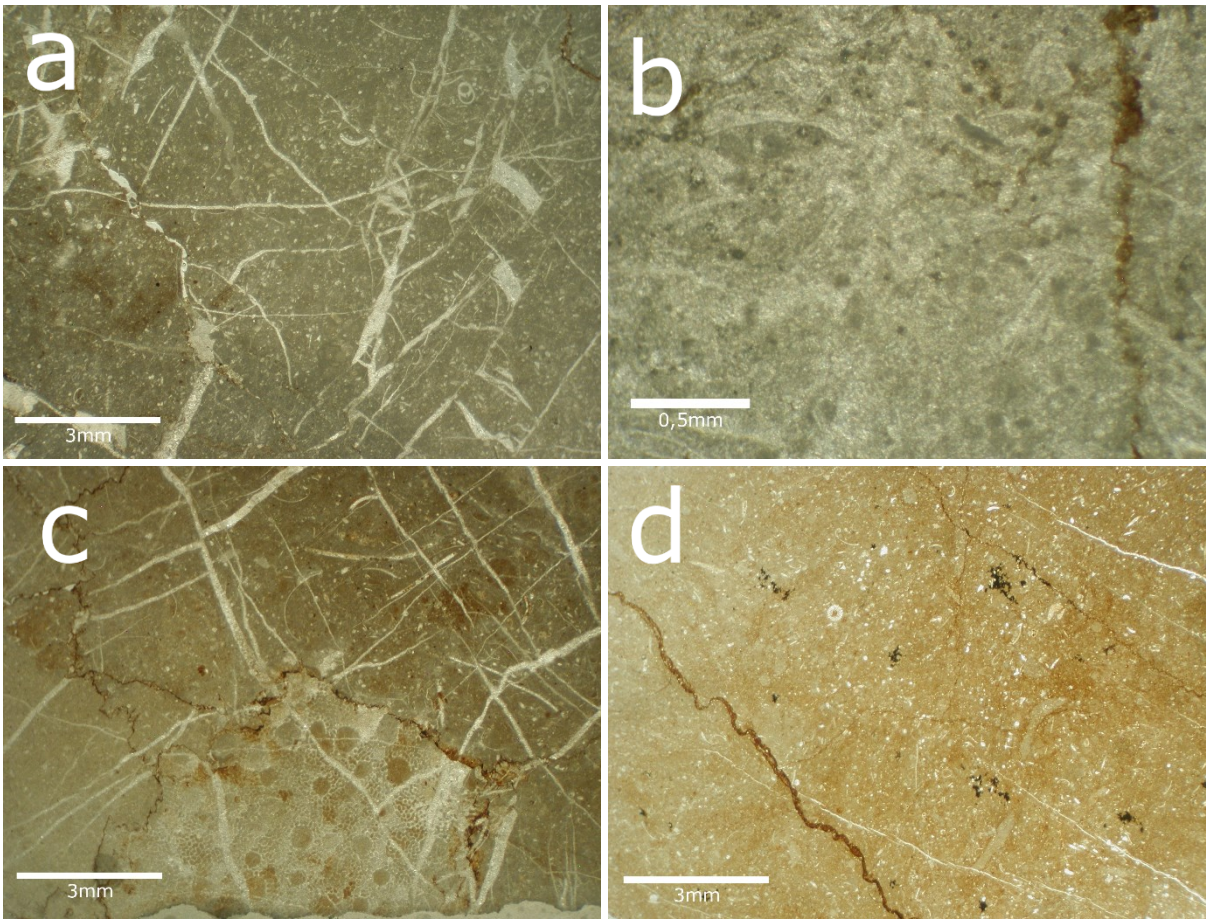

Figure 24: Samples of the Hangendrotkalk, a: Grey - reddish packstone with filaments, some foraminifera and recrystallised radiolarians. The micritic matrix consists of fine-grained bioclasts. Extensional faults are sealed by calcite (sample R45). b: Lumachelle of the Hangendrotkalk show intense recrystallisation (sample R57). c: Reddish – grey bioclastic packstone with small shells, foraminifera and a coral colony show intense styloltization (sample R49). d: Reddish – grey biomicrite packstone with echinoderms, foraminifera and some recrystallised radiolarians show condensed conditions with microbial hard ground formation (sample LA21f).

More radiolarian and ostracod rich limestones belong to the Hangendgraukalk (Figure 25). A hemipelagic outer shelve margin setting of these condensed sediments is clearly visible. Foraminifera, gastropods, echinoderms, as well as holothurians are also found within the samples.

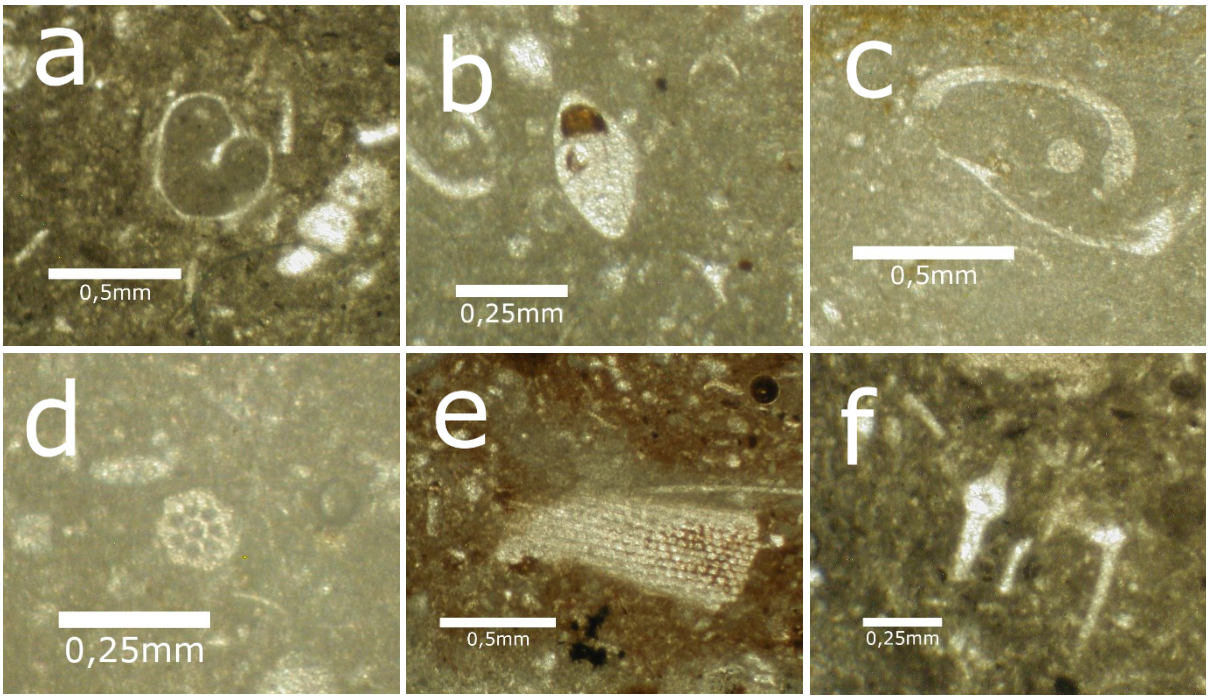

Figure 25: Microfacies table of the Hangendgraukalk with a: Gastropod (sample LA1d), b: Calcite shell of a foraminifera (sample R53), c: Ostracod (sample R54), d: Holothurian (sample R42), e: Echinoderm (sample R52), f: Recrystallised radiolarians (sample LA1d).

The monomict breccias with foraminifera, ostracods, echinoderms, some recrystallised radiolarians and small shells show microbial crusts along the edges of the components (sample R53). The conodont assemblage of *Norigondolella steinbergensis* (Mosher, 1968), *Misikella hernsteini* (Mostler, 1967)*, Epigondolella bidentata* (Mosher, 1968) and *Oncodella paucedentata* (Mostler, 1967) indicates an Early Rhaetian age. An identical matrix between the components indicates sedimentation within an extensional regime. Organic rich limestones show slight bioturbation (sample LA1d).

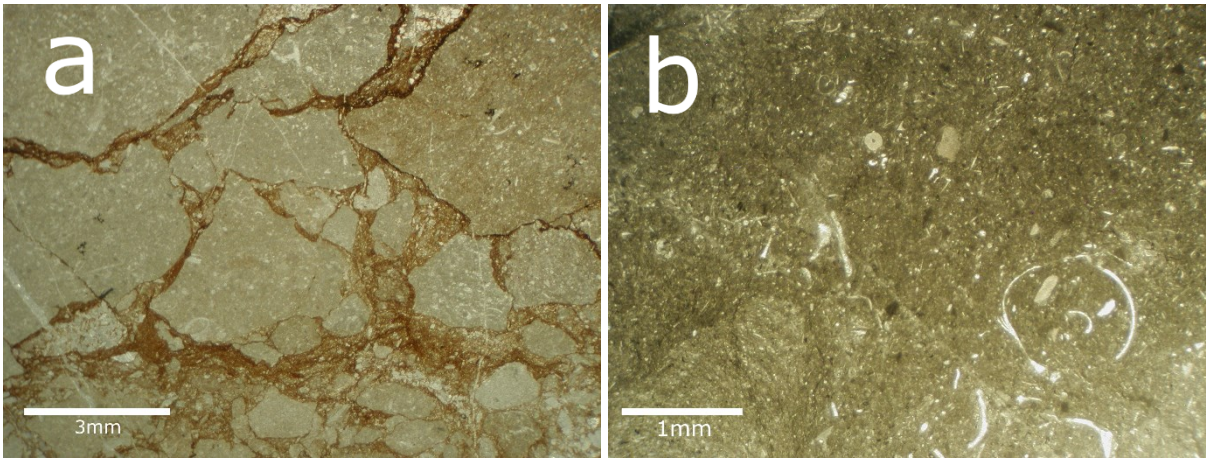

Figure 26: Samples of the Hangendgraukalk. a: Monomict breccia of reddish - grey bioclastic limestone (sample R53). b: Dark grey bioclastic packstone with ostracods, gastropods, crinoids, recrystallised radiolarians and shell fragments (sample LA1d). The matrix consists of organic rich carbonate mud.

4.2.1.4 Dürrnberg Fm.

The radiolarian and spicula rich cherty limestone occur as breccia components within turbidites or mass flow deposits (Figure 27). According to Gawlick et al. (2001, 2009), these samples are countered to the Hettangian to Sinemurian Dürrnberg Fm. Typical is a marly and partly oxidised organic rich matrix with crinoids and radiolarians in between (sample LA21g). A gradual transition from dark and organic rich parts to reddish-oxidised parts reflect the oxygen conditions after deposition. Dark portions within the oxidised parts along faults and breccia components can be identified as migrated organic matter. These faults cut the whole sample and are sealed again by calcite.

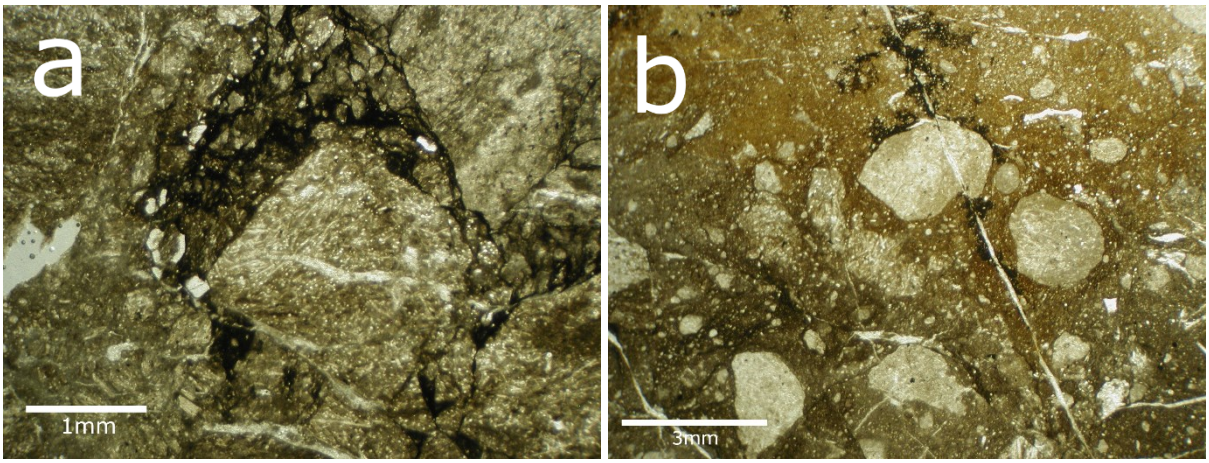

Figure 27: Samples of the Dürrnberg Fm. within the Hengstpass Hallstatt mélange. a: Monomict breccia of dark-grey cherty limestone with an organic rich matrix. Most radiolarians and spicula are recrystallised to calcite (sample LA21g). b: Turbidite breccia of cherty limestone components within a marly matrix containing small radiolarians and crinoid fragments (sample LA21g).

4.2.1.5 Age of the matrix

The argillaceous and siliceous matrix of the Hengstpass Hallstatt mélange includes several radiolarites that slightly differ from each other by their composition (Figure 30). The age determination shows a depositional range from Middle Bathonian to Late Oxfordian, shown in

Figure 28 and Figure 29. Brownish radiolarian turbidites include coarse and silicified breccia components at the base, within a marly matrix and radiolarian mud on top (sample LA22). Some components can be identified as former crinoid fragments or radiolarites. These turbidites show microbial hard ground formation on top of the semi lithified layer. Red radiolarites of a clayey matrix instead show intense bioturbation (sample R41, SD1b). Therefore, lower sedimentation rates are assumed within these types of radiolarites.

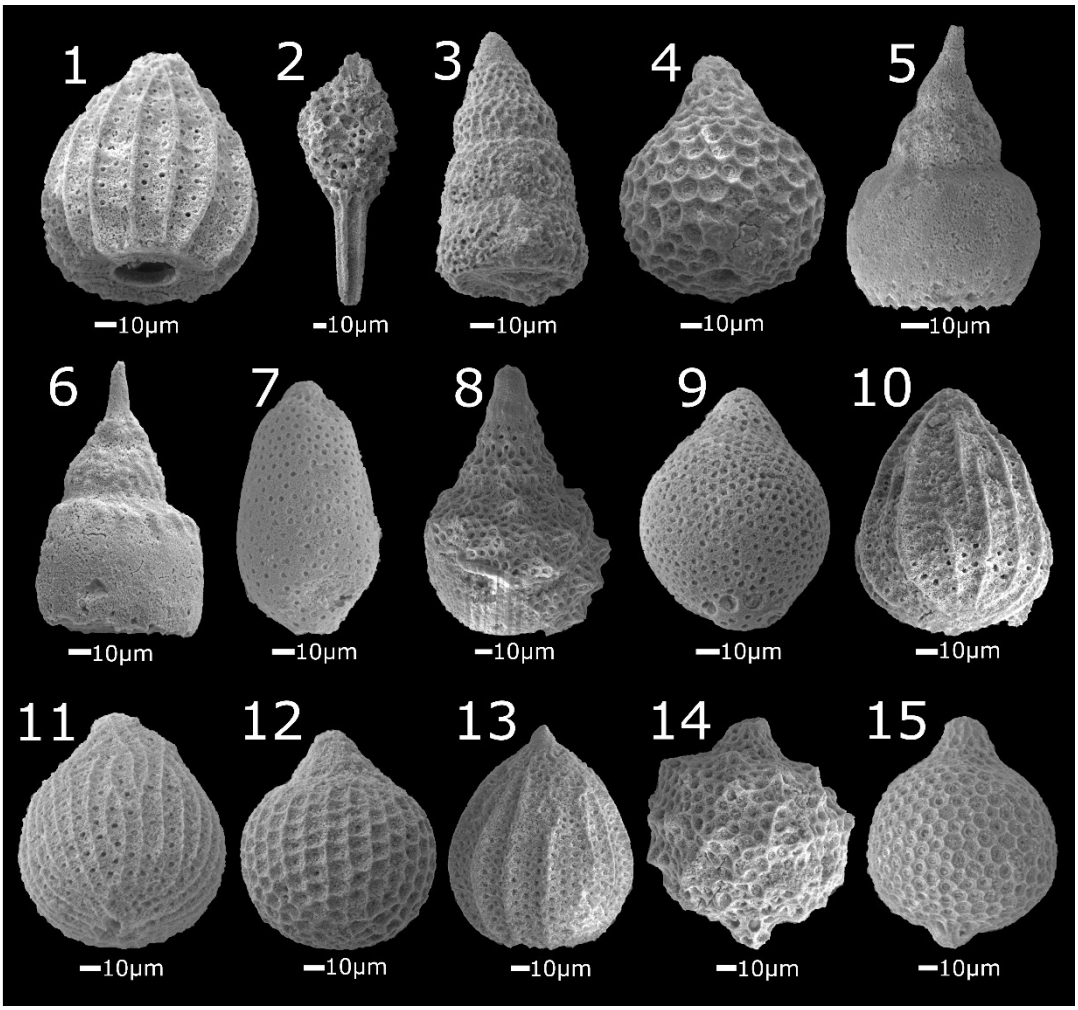

Figure 28: Middle Bathonian to Early Oxfordian radiolarians representing the earliest possible sedimentation of the mélange matrix (sample R17). The age is constrained by 1: *Archaeodictyomitra amabilis* (Aita, 1987), 2: *Archaeospongoprunum sp.,* 3: *Cinguloturris cf. carpatica* (Dumitrica, 1982), 4: *Dictyomitrella kamoensis* (Mizutani & Kido, 1983), 5*: Eucyrtidiellum unumaense* (Yao, 1979), 6: *Eucyrtidiellum unumaense dentatum* (Baumgartner, 1995), 7*: Guexella nudata* (Kocher, 1980), 8: *Hiscocapsa magniglobosa* (Aita, 1987), 9: *Japonocapsa aff. fusiformis* (Yao, 1979), 10: *Protunuma lanosus* (Ozvoldova in Sykora & Ozvoldova, 1996), 11: *Striatojaponocapsa plicarum* (Yao, 1979), 12: *Tricolocapsa tetragona* (Matsuoka, 1983), 13: *Unuma typicus* (Ichikawa & Yao, 1976), 14: *Williriedellum formosum* (Chiari, Marcucci & Prela, 2002), 15: *Williriedellum marcucciae* (Cortese, 1993).

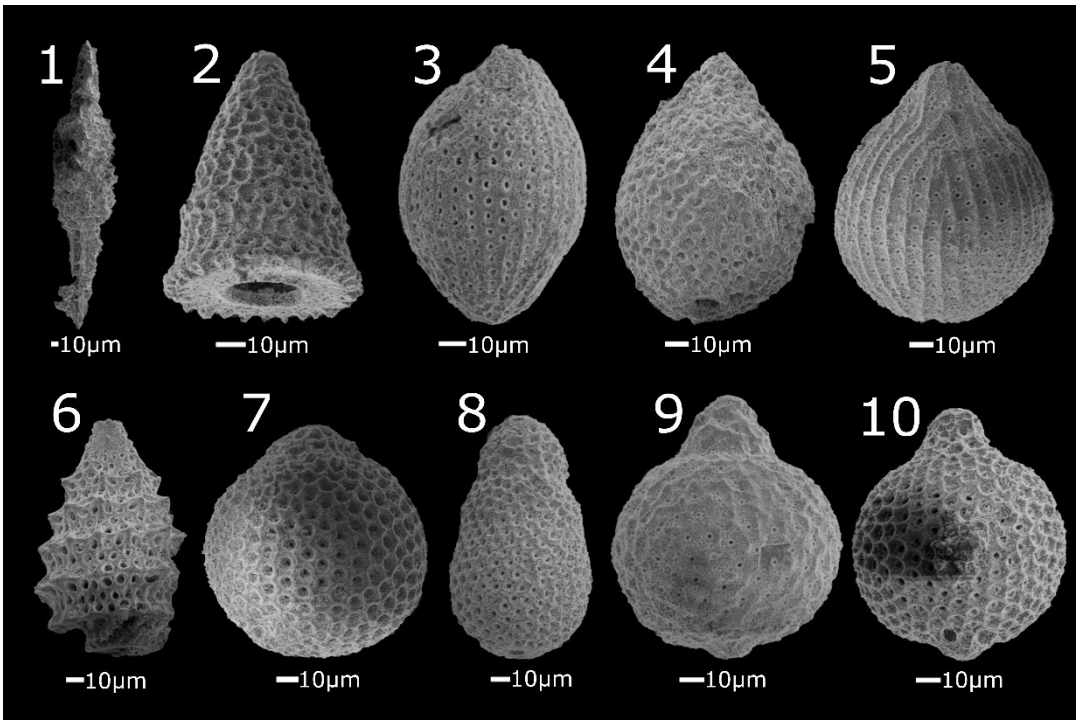

Figure 29: Middle Callovian to Late Oxfordian radiolarians from the Hengstpass Hallstatt Mélange (sample R22). 1: *Archaeospongoprunum cf. elegans* (Wu, 1993), 2: *Dictyomitrella kamoensis* (Mizutani & Kido, 1983), 3: *Helvetocapsa matsuokai* (Sashida, 1999), 4: *Stichocapsa cf. robusta* (Matsuoka, 1984), 5: *Striatojaponocapsa plicarum* (Yao, 1979), 6: *Takemuraella hungarica* (Kozur, 1985), 7*: Tetracapsa cf. himedaruma* (Aita, 1987), 8: *Tricolocapsa sp. S* (Baumgartner et al., 1995), 9: *Williriedellum dierschei* (Suzuki & Gawlick, 2004), 10: *Williriedellum marcucciae* (Cortese, 1993).

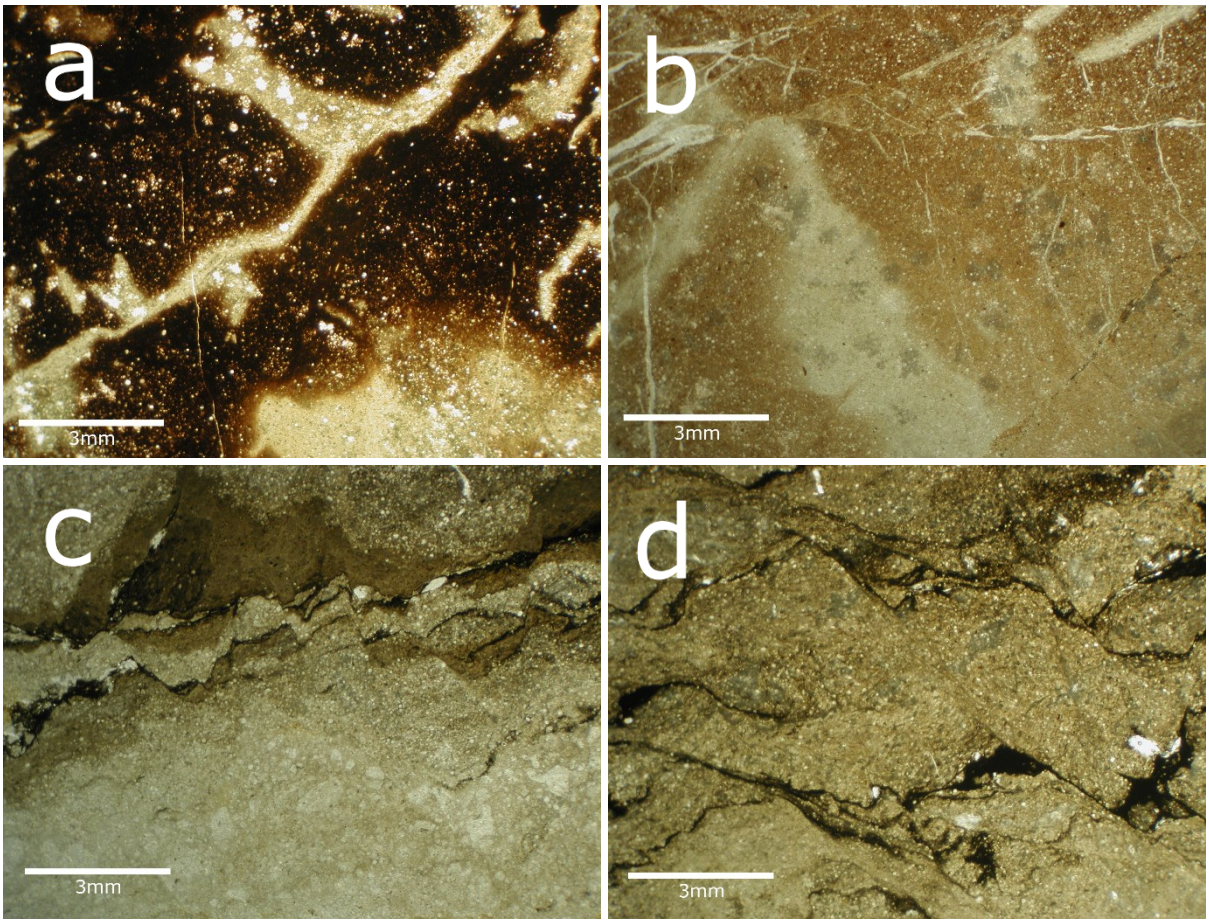

Figure 30: Different radiolarites of the mélange matrix. a: Reddish - green radiolarian packstone. Colourisation is determined by oxidation conditions of the Fe-Mn rich sediment (sample R41). b: Reddish-brown radiolarite. Light portions show a diagenetic overprint by complete silicification (sample LA1b). c: Turbidite of silicified breccia components at the base within a marly matrix and radiolarite mud on top. Some components can be identified as former crinoid fragments or radiolarites. Turbidites show microbial hard grounds formation on top of the semi lithified layer (sample LA22). d: Radiolarian mud with a marly matrix. Dark portions show microbial hard ground formation of the semi lithified turbidites within a slowly transported regime (sample LA22).

4.2.1.6 Older radiolarites

Radiolarites are overgrown by microbial pyrite crusts indicating extreme low sedimentation rates (Figure 31). Such conditions do not occur during mélange sedimentation. Therefore, these radiolarites are supposed to have formed earlier, even if no exact radiolarian ages are present. Sample LA21i also contains microbial pyrite, but the recrystallisation of the radiolarians suggest a diagenetic overprint.

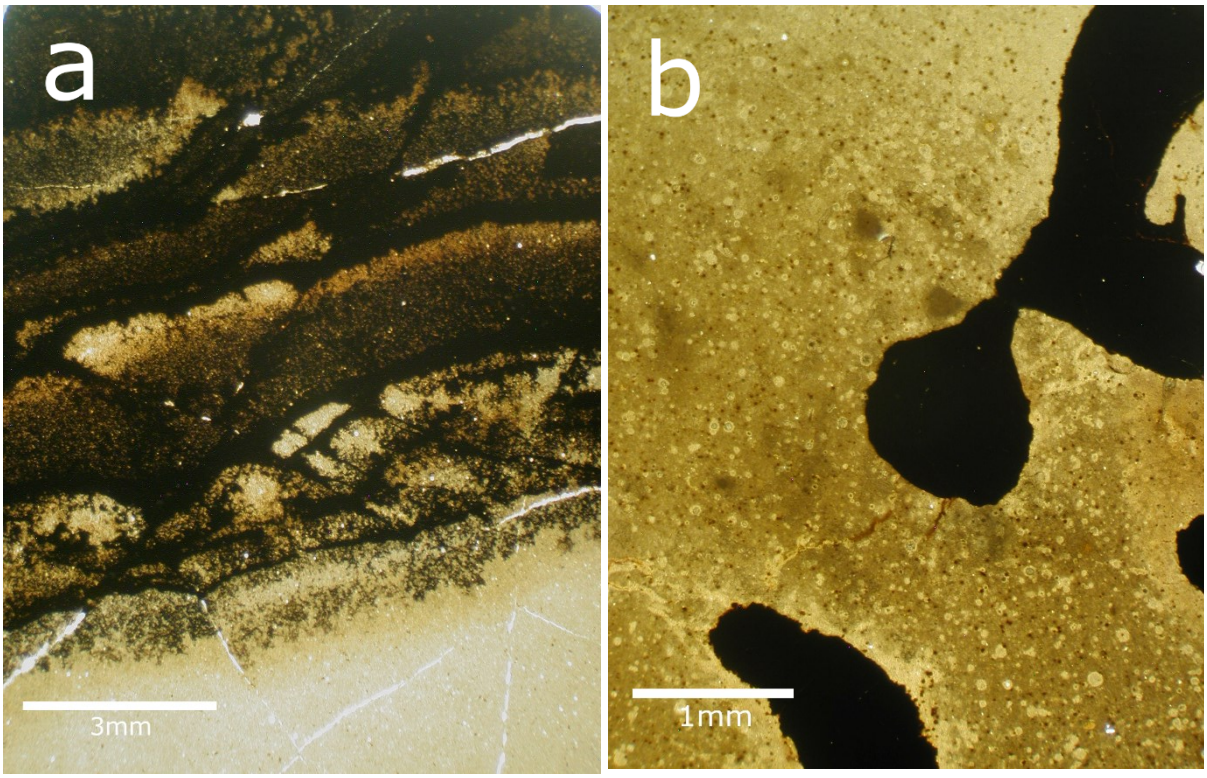

Figure 31: Radiolarites who do not belong to the mélange matrix. a: Carbonate micrite with some tiny radiolarians, overgrown by microbial pyrite formation (sample R40). b: Bioturbated radiolarian wackstone with microbial pyrite. Radiolarians are completely recrystallized to calcite (sample LA21i).

4.2.2 Sealing of the mélange

The Plassen Limestone of the Hengstpass Hallstatt mélange represents a basinal evolution and the sealing of the underlaying mélange by the progradation of the carbonate platform. According to the microfacies, a Kimmerigian to Tithonian age is confirmed (Figure 32).

A shallowing trend is clearly visible within the reconstructed profile of the Schafkogel (see Figure 33). The lower part starts with radiolarian and saccoma limestones with high siliciclastic input (sample R60, R61, R82, R83) passing into more carbonate dominated layers (sample R62-R64) and pure carbonates with shallow-water detritus (sample R65-R68) on top. The progradation of the carbonate platform is clearly visible by the coarsening trend. The upper part again begins with an increase of siliciclastic input, characterised by the samples R69-R75. Alternating carbonates of a deeper facies (sample R76, R78) turning successively into shallower portions (sample R80, R77), reflecting the interplay of sea- level changes and the progradation of the carbonate platform.

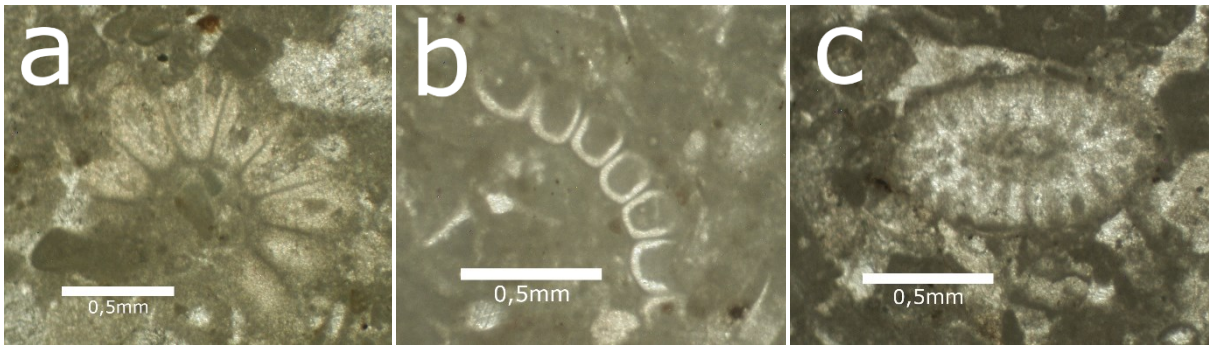

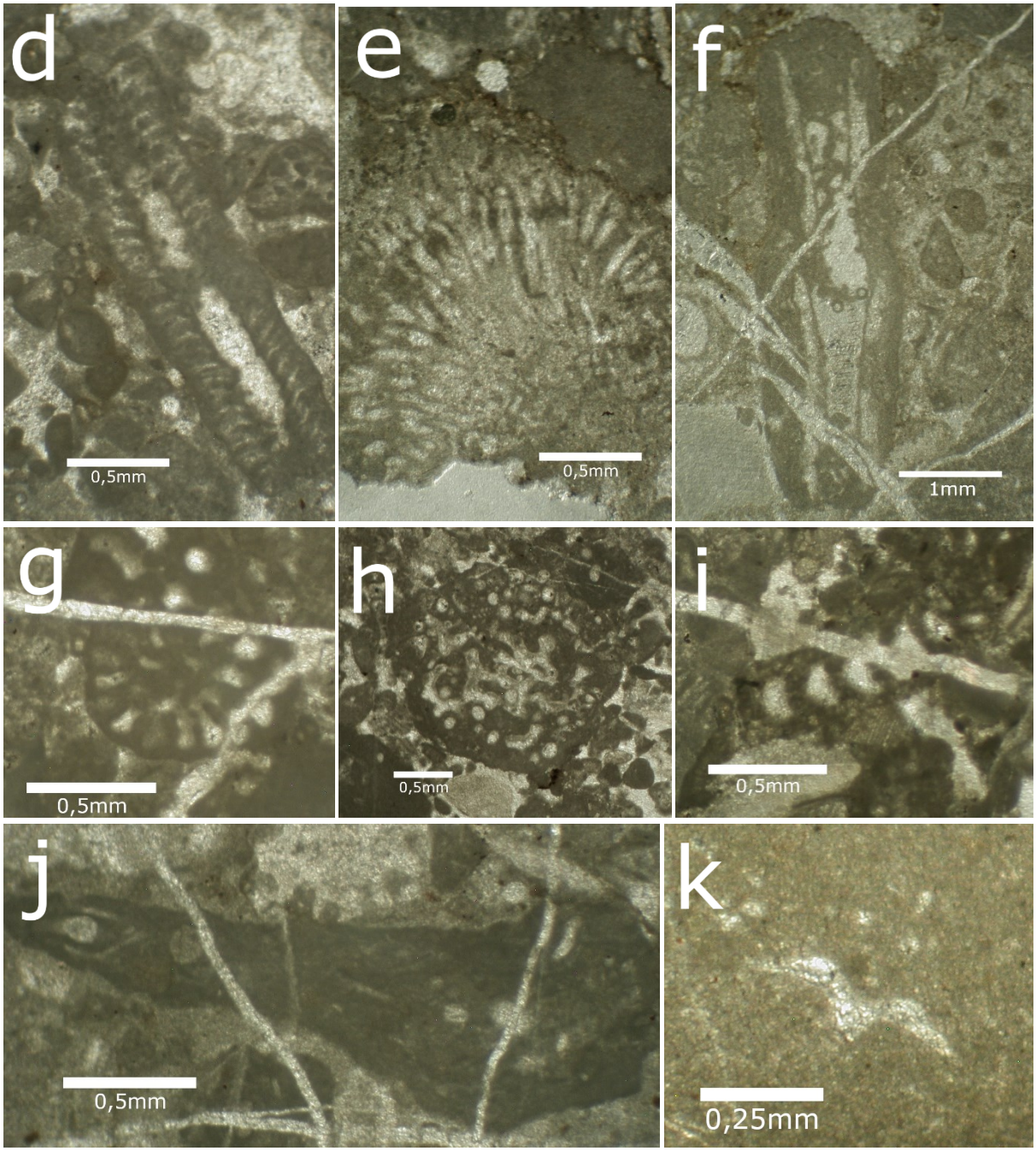

Figure 32: Microfacies table of the Plassen Limestone. a-b: *Aloisalthella sulcata* (Alth, 1882) - sample R80, R62, c-d: *Salpingoporella pygmaea* (Gümbel, 1891) - sample R87, R80, e: *Rivulariaceae -type cyanobacteria* (Bornet & Flahault, 1886) - sample R65, f: *Campbelliella striata* (Bernier, 1974; Carozzi, 1954) - sample R65, g: *Neokilianina rahonensis* (Foury & Vincent, 1967) - sample R87, h: *Coscinophragam* - R87, (Thalmann, 1951) - sample R87, i: *Lituola? baculiformis* (Schlagintweit & Gawlick, 2009) - sample R87, j: *Crescentiella morronensis* (Crescenti, 1969) - sample R66, k: *Saccocoma* - sample R83.

Characteristic is the high amount of siliciclastic material within the carbonate matrix, visible by the brownish colore. All samples show a turbiditic origin and resedimentation within a depositional environment, indicationg a deep-water basin. Radiolarians and crinoids are the dominant fossil framework, especially in fine grained turbidites. Instead, coarser grained packstones show a variety of fossil frameworks including corals, crinoids, brachiopods as well as different algae and foraminifera. The facies integration indicates a transition from lagunal to slope facies, reflecting the progradaton of the carbonate platform and resedimentation of the components.

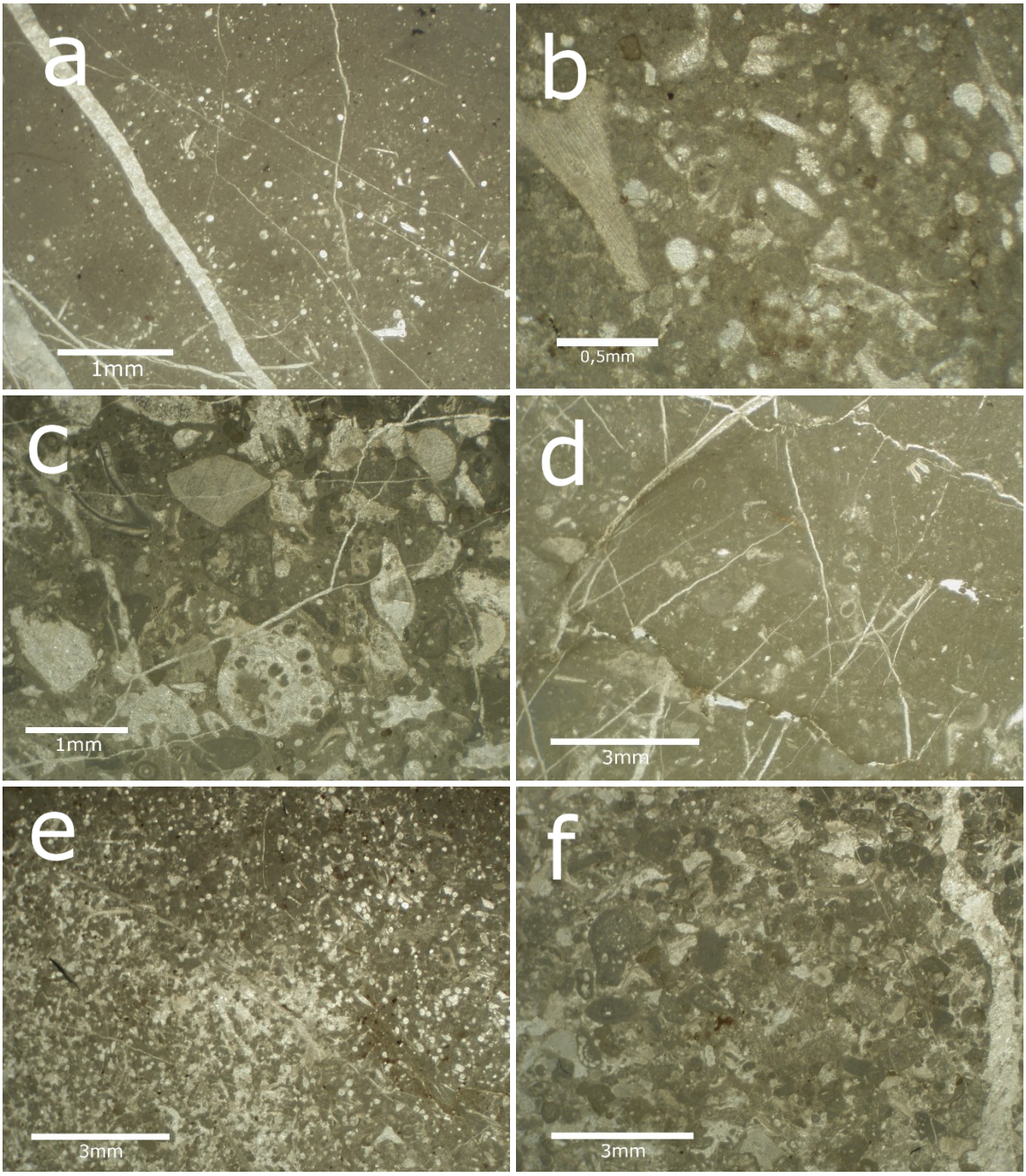

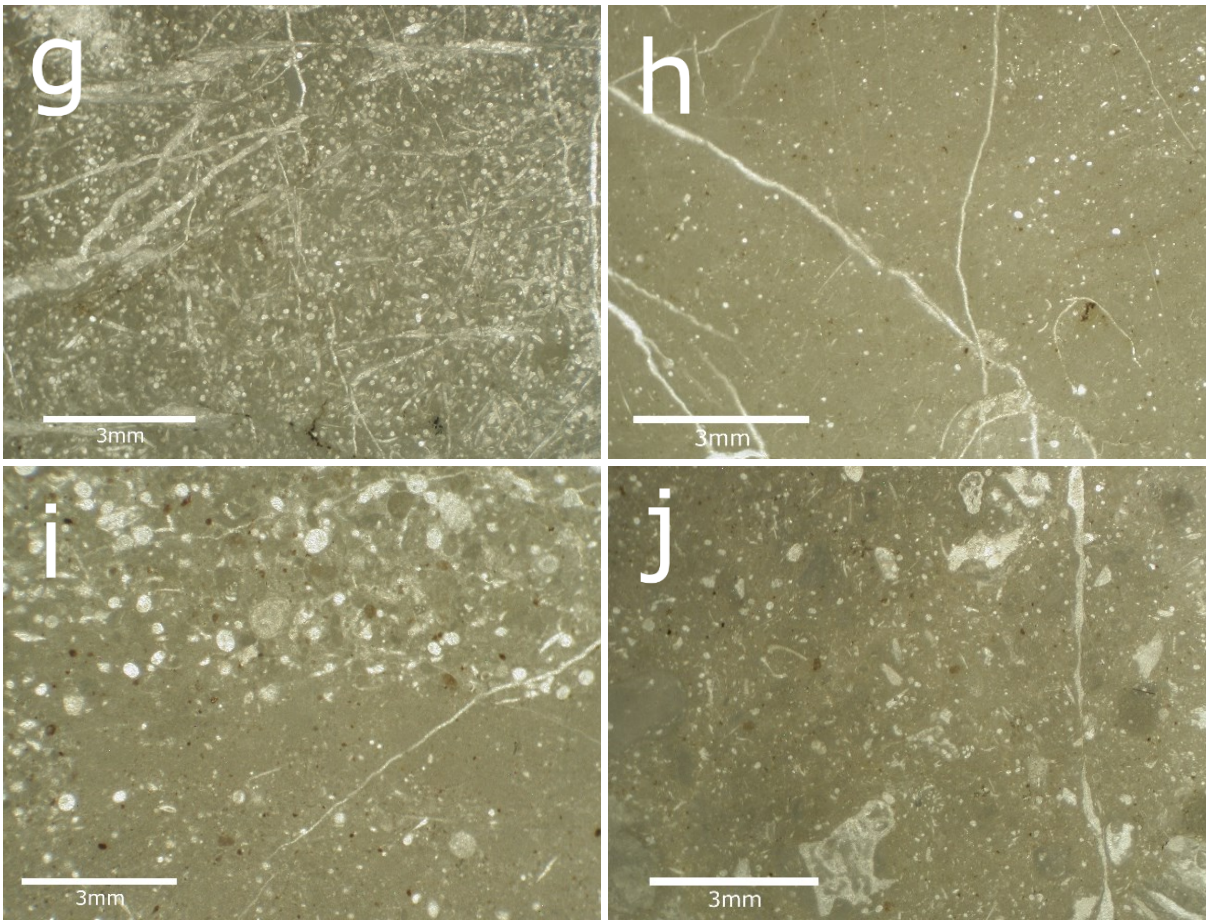

Figure 33 shows the characteristic samples of the reconstructed Schafkogel profile. a: Bioclastic wackstone with radiolarians, saccocoma and few textularid foraminifera. The matrix consists of carbonate mud with increased siliciclastic input (sample R82). b: Bioclastic packstone with radiolarians, echinoderms, foraminifera and algae within a slightly siliciclastic matrix of carbonate mud (sample R63). c: Packstone with crinoids, tubithytes, foraminifera, algae, corals and other reef fragments (sample R66). d: Bioclastic packstone with foraminifera, algae (*Aloisalthella sulcate* - Alth, 1882), crinoids and reef fragments within a matrix of carbonate mud (sample R74). e: Bioclastic packstone of radiolarians, foraminifera, ostracod fragments, some crinoids and saccocoma. The lower part of the turbidite is cemented by sparitic calcite and the upper part consists of a micritic matrix. Little input of siliciclastic material is present in the upper part as well (sample R81). f: Packstone with crinoids, foraminifera (*Protopeneroplis striata* - Weynschenk, 1950), algae and reef fragments (sample R80). g: Radiolarian and saccocoma packstone with a micritic carbonate matrix (sample R79). h: Bioclastic wackstone with some radiolarians in between. The matrix consists of slightly siliceous carbonate mud (sample R76). i: Bioclastic wack - packstone with radiolarian, foraminifera and saccocoma. Clearly visible is the contact between two turbidite layers by the abrupt coarsening of the components (sample R78). j: Bioclastic floatstone with radiolarians, foraminifera (*Redmondoides lugeoni* - Septfontaine, 1977), gastropods, algae and crinoids. The brownish carbonate matrix shows increased siliciclastic input (sample R77).

Beside the profile, carbonate turbidites of shallow water detritus also contain radiolarite components of the underlaying mélange (Figure 34). This characterises the transition from mélange formation to the sealing carbonates. Calcareous algae like *Salpingoporella pygmaea* (Gümbel, 1891) and shallow water foraminifera of the species *Protopeneroplis striata* (Weynschenk, 1950) are common within the sample. Incrusted reef organisms also confirm the platform derived material.

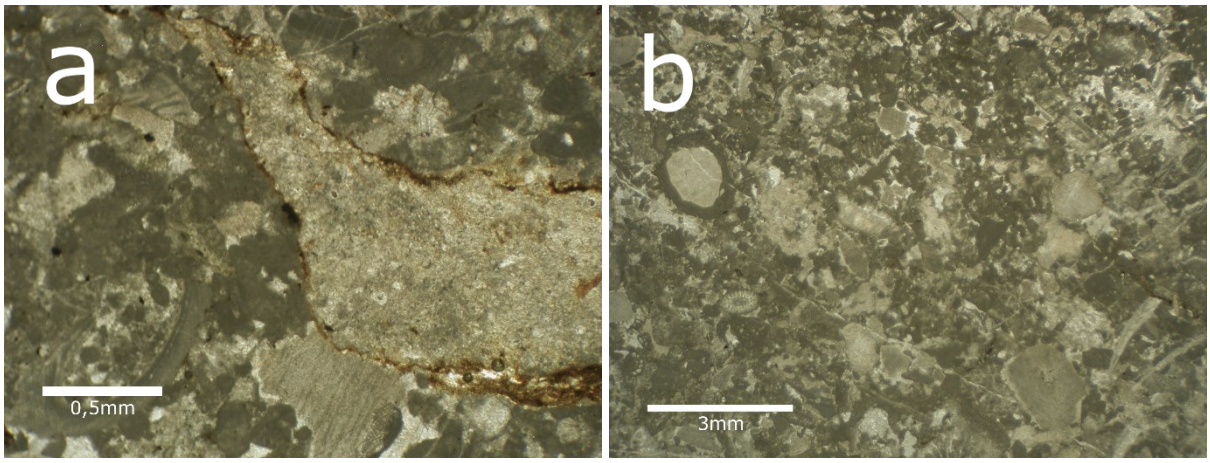

Figure 34: shows a: radiolarite fragment within the crinoid rich bioclastic rudstone (sample R87) and b: bioclastic rudstone with algae (*Salpingoporella pygmaea* - Gümbel, 1891), crinoids, foraminifera (*Protopeneroplis striata* - Weynschenk, 1950), corals and reef fragments. Some bioclasts show microbial incrustation (sample R87).

5 Interpretation of the results

5.1 Jaklovce

Based on the previous investigations from the Jaklovce section, the affinity of the sedimentary succession to the ocean floor is confirmed. The transition of basalts (analysed by Putiš et al., 2019) to the sedimentary cover represents the typical upper part of the so-called Steinmann-Trinity (Steinmann, 1925; Bernoulli et al., 2003). Greenschist facies ocean floor metamorphism led to the formation of chlorite, actinolite, epidote and albite. Excess of iron is compensated by the formation of magnetite.

The sedimentary succession is directly correlated with the break-up of the Neo-Tethys Ocean and the associated volcanism in the Late Anisian (Haas et al., 2011). This is represented by massive volcanic ash layers in the lower part of the profile. Open-marine siliceous sedimentation dominated especially in the most distal facies belts (Meliata facies zone). The appearance of *Muelleritortidae* (Kozur, 1988) in the middle part of the succession fits well within this time. The Wetterstein Carbonate platform established in the Late Ladinian and during the Early Carnian rapid aggradation sheds little amounts of carbonate also in the Meliata facies zone. This can be recognised by a slight carbonate increase in some beds of the middle part. The appearance of *Xiphothecaella rugosa* (Bragin, 1991) within the uppermost part indicates at least a Late Carnian age and also confirms the orientation of the sedimentary succession beside the correlation with the sedimentation conditions within the time of deposition. The increased carbonate content can also be correlated with the Late Carnian onset of the Dachstein Carbonate Plattform. These results are in contrast with the orientation of the sedimentary succession of Putiš et al. (2019), who turned the profile around.

5.2 Raucherschober/Schafkogel

With consideration of the research of (Plöchinger & Prey, 1968), parts of the Neo-Tethys distal continental margin from the Early Triassic onward could be reconstructed within the Hengstpass Hallstatt mélange. The early stage of the Neo-Tethys Wilson-Cycle is represented by the occurrence of Werfener beds, and the distal shelf of the Neo-Tethys continental margin is characterised by condensed sedimentation of the Hallstatt Limestone. Radiolarian and spicula rich limestones of the Dürrnberg Fm. also appear as components within mass transported deposits. Ferrous microbial crusts are the result of extreme condensed conditions caused by the extension and the formation of a horst and graben morphology in Early Jurassic times.

Even if the sampled basalt of the Hengstpass Hallstatt mélange do not show similar geochemical composition as those of the Jaklovce mélange blocks (see Putiš et al., 2019), the calc-alkaline volcanic arc affinity is clearly visible and define the rock as arc related basalt. In this case, this basalt is interpreted as the product of intra oceanic subduction and the formation of an early arc at the beginning ophiolite obduction in early Middle Jurassic times. This favours the model of multiple stacked ophiolite nappes thrust over the Neo-Tethys continental margin instead of a single thrust sheet. Hydrothermal alteration caused leaching of the elements Si, Al, and Na and a concentration of Fe, Ti, K and Mg. The abnormal high Ca content is explained as the result of intense alteration of Ca-rich solutions, derived from the surrounding mélange components and the overlaying Plassen Limestone.

All these relics of various Triassic to Middle Jurassic limestones, radiolarites and rocks from the ophiolite suite lay within a Middle to early Late Jurassic radiolaritic – argillaceous matrix, forming deep-water basin fills of the propagating ophiolites. These mélanges are later sealed by the progradation of the Plassen Limestone at a time of decreased tectonic in the Late Jurassic, shown by the shallowing trend of the Schafkogel profile.

5.3 Comparison with Regional Framework

All these relics of various Triassic limestones, radiolarites and rocks from the ophiolite suite laying within an earliest Late Jurassic radiolaritic - argillaceous matrix (Kozur & Mostler, 1992; Mandl & Ondrejičková, 1993; Kozur et al., 1996; Mock et al., 1998), combining them as derived from the same ocean system and sharing the same tectonic evolution till the Late Jurassic. Therefore, the one-ocean model from Bernoulli & Laubscher (1972) and ongoing ophiolite obduction onto the wider Adriatic shelf margin is supported.

Similar mélanges are investigated in the Hellenides, Albanides and Dinarides (Bortolotti et al., 1996; Chari et al., 2011; Ozsvart et al., 2012; Gawlick & Missoni, 2019), from the Pelso unit (Kovács et al., 2010; Ozsvart & Kovács, 2012) and the Kalnur unit north of the mid Hungarian fault belt (Haas & Kovács, 2012). From the Inner Western Carpathians they are described by (Mandl & Ondrejičková, 1991; Kozur & Mostler, 1992; Mandl & Ondrejičková, 1993; Mandl, 1996; Neubauer et al., 2007). These ophiolitic mélanges contain the reworked Middle Triassic to Middle Jurassic ophiolite suite and there overlaying sedimentary cover. The type locality Meliata s. str. also include blocks from the distal Neo-Tethys continental margin (Cekaltova, 1954; Mock, 1980; Kozur & Mock, 1985, 1995; Mock et al., 1998; Aubrecht et al., 2012; Gawlick & Missoni, 2015). Instead, the Jaklovce mélange shows the most distal depositional environment of the ocean floor (Kozur & Mock, 1985; Mock et al., 1998; Putiš et al., 2019; Putiš, 2020). The affinity of basalts and the overlaying siliceous sedimentary

cover clearly define these rocks as the uppermost part of the so called Steinamnn-Trinity. Therefore, the Jaklovce mélange is defined as ophiolitic mélange.

Sedimentary mélanges, mainly consisting of components derived from the outer shelf region (Hallstatt facies zone), are instead classified as Hallstatt Mélange. Within the Northern Calcareous Alps, none of these mélanges contain basaltic material. Only the investigated Raucherschober and Schafkogel revealed below the Late Jurassic Plassen Limestone ophiolitic material. Therefore, the Hengstpass Hallstatt mélange becomes crucial for the paleogeographic and geodynamic reconstruction of this area.

In this case, the following geodynamic history is supported (see Figure 35): From Late Permian on, the W-Tethyan realm was affected by extension that caused rapid subsidence and the subsequence formation of a passive continental margin setting. With the final break-up of the Neo-Tethys Ocean in Late Anisian times this margin setting reached its completion. A trend to more siliceous sedimentation can be recognized in all facies belts, even in the most distal parts (Meliata facies zone). With ongoing ocean spreading, the carbonate production recovered and the typical passive continental margin emerged. The change from extension to compression in Early Jurassic times resulted in subsidence in the outer shelf regions, indicating the beginning of intra oceanic subduction and ophiolite obduction. This event is directly connected with the formation of subduction related volcanic rocks. The calc-alkaline arc affinity of the basalt from the Schafkogel also formed in this process.

From this time on, trench like basins formed in front of the propagating nappes, which are filled with the erosional products of the ophiolites and the former passive continental margin. The Adriatic shelf now attained a lower plate position in relation to the obducted ophiolites. These mass transport deposits, containing blocks of various size within a radiolaritec-argillaceous matrix showing a coarsening upward trend and are dragged along to the upper regions of the continental margin. In a period of decreased tectonic activity, carbonate platforms established around the Oxfordian/Kimmeridgian on top of the obducted ophiolites (Carras et al., 2004; Schlagintweit et al., 2008) or on top of the different nappe fronts of the newly formed nappe stack (Kukoč et al., 2012 with references therein). The deep-water basins containing the sedimentary mélange are sealed by the progradation of these carbonate platforms, also known as Plassen Carbonate platform.

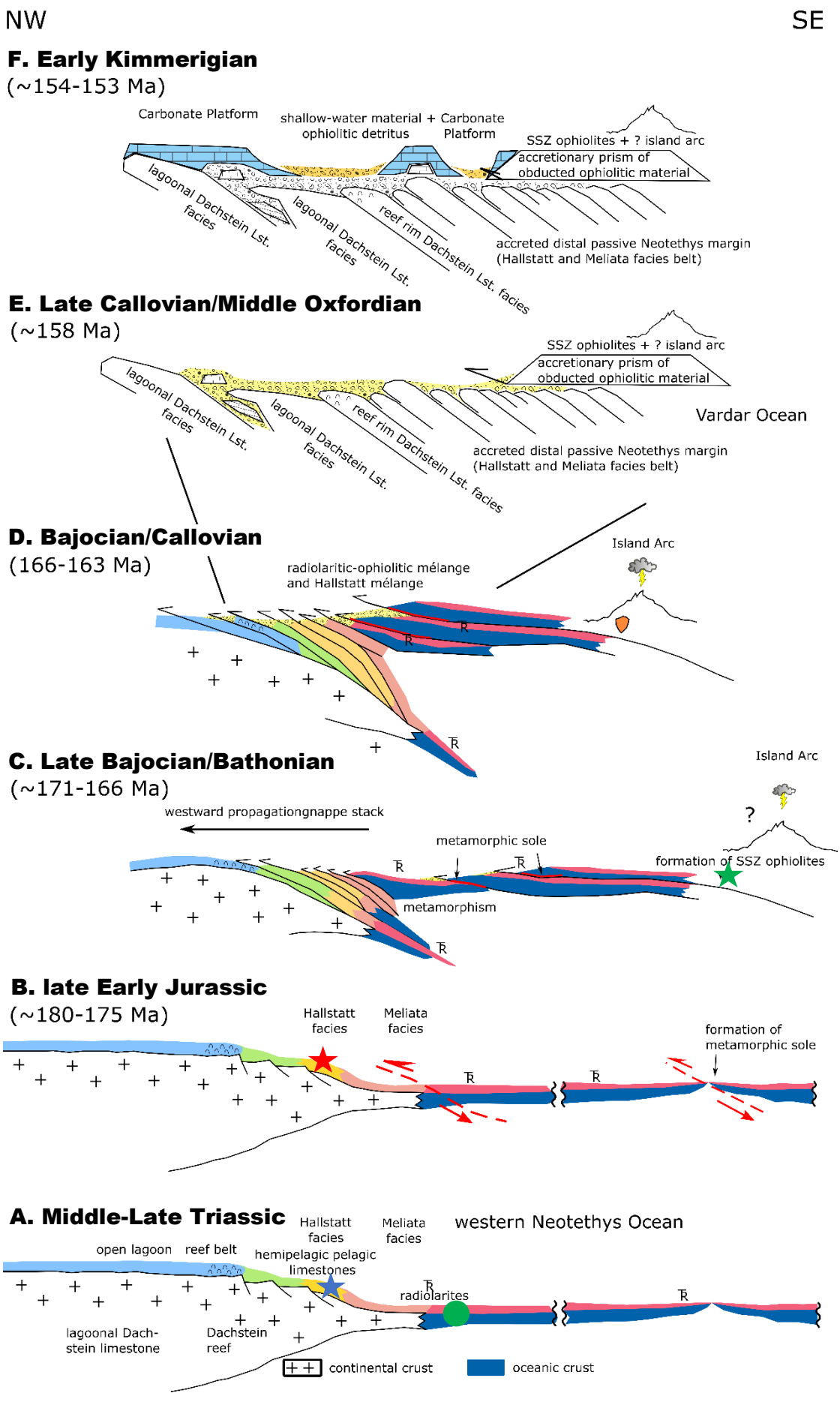
NW
SE
F. Early Kimmerigian
(~154-153 Ma)
Carbonate Platform
shallow-water material + Carbonate ophiolitic detritus
Platform
SSZ ophiolites + ? island arc
accretionary prism of obducted ophiolitic material
lagoonal Dachstein Lst. facies
lagoonal Dachstein Lst. facies
reef rim Dachstein Lst. facies
accreted distal passive Neotethys margin (Hallstatt and Meliata facies belt)
E. Late Callovian/Middle Oxfordian
(~158 Ma)
SSZ ophiolites + ? island arc
accretionary prism of obducted ophiolitic material
lagoonal Dachstein Lst. facies
lagoonal Dachstein Lst. facies
reef rim Dachstein Lst. facies
Vardar Ocean
accreted distal passive Neotethys margin (Hallstatt and Meliata facies belt)
D. Bajocian/Callovian
(166-163 Ma)
radiolaritic-ophiolitic mélange and Hallstatt mélange
Island Arc
C. Late Bajocian/Bathonian
(~171-166 Ma)
Island Arc
?
westward propagationgnappe stack
metamorphic sole
formation of SSZ ophiolites
metamorphism
B. late Early Jurassic
(~180-175 Ma)
Hallstatt facies
Meliata facies
formation of metamorphic sole
A. Middle-Late Triassic
Hallstatt facies
Meliata facies
western Neotethys Ocean
open lagoon
reef belt
hemipelagic pelagic limestones
radiolarites
lagoonal Dach-stein limestone
Dachstein reef
continental crust
oceanic crust

Figure 35: Modified evolution of the western Neo-Tethys margin since the Middle-Late Jurassic times after (Gawlick et al., 2015, 2016a). The paleogeographic environment for the formation of the different investigated rocks is illustrated with stars and dots of different colors: green dot = Jaklovce basalt and sedimentary cover (Late Anisian - Norian), blue star = Hallstatt Limestone (Raucherschober/Schafkogel), red star = Dürrnberg Fm. and older radiolarites (Raucherschober/Schafkogel), green star = basalt (Raucherschober/Schafkogel). The mélange matrix is illustrated in D and E in light yellow and the Plassen Limestone is illustrated in F in dark yellow. A. Schematic passive continental margin to the Neo-Tethys ocean. B. Transition from extension to compression within the Neo-Tethys occurred in late Early Jurassic times. Bulging of the distal continental margin caused extreme condensed conditions and the formation of ferrous crusts at the outer shelf margin. C. The onset of ophiolite obduction in Bajocian times forced the formation of ophiolitic mélanges in the oceanic realm. D. Ongoing ophiolite obduction results in the formation of trench-like basins in front of the propagating nappe-stack and imbrication of the former passive Neo-Tethys continental margin as sedimentary mélange. E. Overthrusting of the distal nappes by the accretionary prism after tectonic shortening caused sedimentation into the newly formed basins in front. F. Carbonate platforms established on top of the obducted ophiolites, or on top of the different nappe fronts. The enormous carbonate supply sealed the mélange basins.

6 Conclusion

The sedimentation of the oceanic derived Jaklovce succession continued from the Ladinian to at least Late Carnian (Putiš et al., 2019). The association of basalts and siliceous cover sediments represent the typical Steinmann-Trinity of the ocean-floor. Therefore, this mélange blocks represent one of the oldest remnants of the Neo-Tethys ocean-floor, deposited relatively near to the continental margin. The age determination, as well as the correlation with the reconstructed sedimentation condition of the distal continental margin led to a re-orientation of the whole block.

Reinvestigation of the Raucherschober and Schafkogel led to a new interpretation of the locality as a Hallstatt mélange which also contains ophiolitic material derived from the accretion of the Neo-Tethys margin. Therefore, a new mélange within the Northern Calcareous Alps is found containing ophiolitic material. The volcanic arc affinity of the basalt at the Schafkogel supports a multiple stacked ophiolite obduction onto the wider Adriatic shelf (Gawlick et al., 2008). Sedimentation of the mélange matrix since Bathonian times heavily favours an early Middle Jurassic nappe stacking (Gawlick & Missoni, 2019). This leads to the following conclusions:

1. By combining all the obtained data from the Jaklovce section, a clear affinity to the Neo-Tethys ocean floor is confirmed. The correlation with the sedimentation conditions within the time of the ocean break-up, as well as the age determinations of a Late Ladinian to at least an Upper Carnian sedimentation period clearly favours the one ocean model.

2. Holding into account that the accretion of the nappe stack caused extreme shortening in NW direction that holds similar components in a narrow belt along the closing ocean does not fit into the large E-W distance between the two investigated areas. In this case, the perception that the Raucherschober and Schafkogel form the thrust complex of the underlaying nappes that are dragged along the front of the Haller Mauer (Kraus, 1944) is not supported. Instead, the theory of Spengler (1959) of an overthrusting Hengstpass Hallstatt mélange is regained. After sealing of the trench-like basins in front of the propagation nappes by carbonate platforms (Schlagintweit & Gawlick, 2007), mountain uplift and subsequent exhumation collapse started in the Late Jurassic (Gawlick & Missoni, 2019). This could drag these similar mélanges to these far distances.

7 Literature

Alth, A. (1882). Die Versteinerungen des Nizniower Kalksteines. *Beitr. Paläont. Oesterr.-Ung, Wien*, *1*, 183–332.

Arkai, P., Faryad, S. W., Vidal, O., & Balogh, K. (2003). Very low-grade metamorphism of sedimentary rocks of the Meliata unit, Western Carpathians, Slovakia: Implications of phyllosilicate characteristics. *International Journal Earth Sciences*, *92*, 68–95.

Aubrecht, R., Gawlick, H.-J., Missoni, S., & Plašienka, D. (2012). Meliata type locality revisited: Evidence for the need of reinvestigation of the Meliata Unit and redefinition of the Meliata Mélange. *Mineralia Slovaca*, *44*, 71.

Aubrecht, R., Gawlick, H.-J., Missoni, S., Suzuki, H., Plašienka, D., Kronome, K., & Kronome, B. (2010). Middle Jurassic matrix radiolarians from the Meliata ophiolitic mélange at the type Meliata sites Meliata and Jaklovce (Western Carpathians): Palaeogeographic evidence. *Journal of Alpine Geology*, *52*, 82–83.

Bernier, P. (1974). Campbelliella striata (CAROZZI), algue dasycladacée? Une nouvelle interprétation de l´organisme « C » FAVRE et RICHARD. *Géobios, Lyon*, *7*(2), 155–175.

Bernoulli, D., & Laubscher, H. (1972). The palinspastic problem of the Hellenides. *Ecl. Geol. Helv.*, *65*, 107–118.

Bernoulli, D., Manatschal, G., Desmurs, L., & Münterer, O. (2003). Where did Gustav Steinmann see the trinity? Back to the roots of an Alpine ophiolite concept. *Geological Society of America, Special Paper*, *373*, 93–110.

Bezák, V., Broska, I., Ivanička, J., Reichwalder, P., & Vozár, J. (2004). Tectonic Map of Slovak Republic 1:500,000, Bezák, V., Ed. *Ministry of the Environment of the Slovak Republic. Bratislava: State Geological Institute of Dionýz Štúr*.

Bornet, É., & Flahault, C. (1886). Revision des Nostocacées hétérocystées contenues dans les principaux herbiers de France. *Annales des Sciences Naturelles, Botanique*, *3*, 323–381.

Bortolotti, V., Kodra, A., Marroni, M., Mustafa, F., Pandolfi, L., Principi, G., & Saccani, E. (1996). Geology and Petrology of ophiolitic sequences in the Mirdita region (Northern Albania). *Ofioliti*, *21*, 3–20.

Bragin, N. Y. (1991). Radiolaria and lower Mesozoic Units of the USSR, east regions. *Trans. Acad. Sci. USSR*, *469*, 1–125.

Cabanis, B., & Lecolle, M. (1989). Le diagramme La/l0-Y/15-Nb/8: Un outil pour la discrimination des séries volcaniques et la mise en évidence des processus de mélange et/ou de contamination crustale. *Comptes Rendus De L'academie Des Sciences, Paris Ser. 2*, *313*, 2023–2029.

Carey, S. W. (1958). The tectonic approach to continental drift. In: Carey, S.W. (Ed.), Continental Drift a Symposium. *Geological Department, University of Tasmania, Hobar*, 177–358.

Carozzi, A. (1954). L´organisme "C" J. Favre (1927) est une Vaginella portlandienne. *Arch.Sci., Genf*, *7*(2), 107–111.

Carras, N., Fazzuoli, M., & Photiades, A. (2004). Transition from carbonate platform to pelagic deposition (Mid-Jurassic-Late Cretaceous), Vourinos massif, northern Greece. *Revista Italiana di Paleontologia e Stratigrafia*, *110*, 345–355.

Cekaltova, V. (1954). Geological setting of southern part of the Slovak Crust (in Slovak). *Geol Prace*, *1*(4), 8–160.

Chari, M., Djeric, N., Garfagnoli, F., Hrvatovic, H., Krstic, M., Levi, N., Malasoma, A., Marroni, M., Menna, F., Nirta, G., Pandolfi, L., Principi, G., Saccani, F., Stojadinovic, U., & Tricic, B. (2011). The geology of the Zlatibor Maljen area (western Serbia): A geotraverse across the ophiolites of the Dinaric-Hellenic collisional belt. *Ofioliti*, *36*, 139–166.

Chiari, M., Baumgartner, P. O., Bernoulli, D., Bortolotti, V., Marcucci, M., Photiades, A., & Principi, G. (2013). Late Triassic, Early and Middle Jurassic Radiolariafrom ferromanganese-chert 'nodules' (Angelokastron, Argolis,Greece): Evidence for prolonged radiolarite sedimentationin the Maliac-Vardar Ocean. *Facies*, *59*, 391–424.

Crescenti, U. (1969). Biostratigrafia delle facies mesozoiche dell´ Apennino Centrale: Correlazioni. *Geol. Romana, Rom*, *8*, 15–40.

Csontos, L. (2006). Chapter 3.5 – Mesozoic stratigraphy of the gemerides. In: Horváth, F., Galácz, A. (Eds.), The Carpathian-Pannonian Region. A Review of Mesozoic- Cenozoic Stratigraphy and Tectonics. *Geologica Pannonica Special Publication*, *1*, 61–83.

Csontos, L., & Vörös, A. (2004). Mesozoic plate tectonic reconstruction of the Carpathian region. *Palaeogeogr Palaeoclimatol Palaeoecol*, *210*, 1–56.

Dallmeyer, R. D., Neubauer, F., & Fritz, H. (2008). The Meliata suture in the Carpathians: Regional significance and implications for the evolution of high pressure wedgeswithin collisional orogens. In: Siegesmund, S., Fügenschuh, B., Froitzheim, N. (Eds.), Tectonic Aspects of the Alpine-Dinaride-Carpathian System. *Geological Society London Special Publications*, *298*, 101–115.

Dimitrijević, M. N., Dimitrijević, M. D., Karamata, S., Sudar, M., Gerzina, N., Kovács, S., Dosztály, L., Gulácsi, Z., Less, G., & Pelikán, P. (2003). Olistostrome/mélanges – an overview of the problems and preliminary comparison of such formations in Yugoslavia and NE Hungary. *Slovak Geological Magazine*, *9*, 3–21.

Dumitrică, P., & Mello, J. (1982). On the Age of the Meliata Group and the Silica Nappe Radiolarites (localities Drţkovce and Bohúňovo, Slovak Karst, ČSSR). *Geol. Práce Spr*, *77*, 17–28.

Faryad, S. W., & Henjes-Kunst, F. (1997). Petrological and K-Ar and 40Ar-39Ar age constraints for the tectonothermal evolution of the high-pressure Meliata unit, Western Carpathians (Slovakia). *Tectonophysics*, *280*, 141–156.

Faupl, P., & Wagreich, M. (2000). Late Jurassic to Eocene palaeogeography and geodynamic evolution of the Eastern Alps. *Mitteilungen Österreichische Geologische Gesellschaft*, *92*, 79–94.

Festa, A., Pini, G. A., Dilek, Y., Ogata, K., & Alonso, J. L. (2016). Origin and significance of olistostromes in the evolution of orogenic belts: A global synthesis. *Gondwana Research*, *39*, 180–203.

Foury, G., & Vincent, E. (1967). Morphologie et répartition stratigraphique du genre Kilianina PFENDER (Foraminifère). *Eclogae geol. Helv., Basel*, *60*(1), 33–45.

Frank, W., & Schlager, W. (2006). Jurassic strike slip versus subduction in the Eastern Alps. *International Journal of Earth Sciences*, *95*, 431–450.

Frisch, W., & Gawlick, H.-J. (2003). The nappe structure of the central Northern Calcareous Alps and its disintegration during Miocene tectonic extrusion—A contribution to understanding the orogenic evolution of the Eastern Alps. *International Journal of Earth Sciences*, *92*, 712–727.

Frisch, W., Meschede, M., & Blakey, R. (2011). Plate Tectonics. *Springer*, 212.

Froizheim, N., Plašienka, D., & Schuster, R. (2008). Alpine tectonics of the Alps and Western Carpathians. In: McCann, T. (Ed.), The Geology of Central Europe. *The Geological Society, London*, 1141–1232.

Gawlick, H.-J., Aubrecht, R., Schlagintweit, F., Missoni, S., & Plašienka, D. (2015). Ophiolitic detritus in Kimmeridgian resedimented limestones and its provenance from an eroded obducted ophiolitic nappe stack south of the Northern Calcareous Alps (Austria). *Geologica Carpathica*, *66*, 473–487.

Gawlick, H.-J., & Böhm, F. (2000). Sequence and isotope stratigraphy of Late Triassic distal periplatform limestones from the northern Calcareous Alps (Kälberstein Quarry, Berchtesgaden Hallstatt Zone). *International Journal of Earth Science*, *89*(1), 108–129.

Gawlick, H.-J., Frisch, W., Hoxha, L., Dumitrica, P., Krystyn, L., Lein, R., Missoni, S., & Schlagintweit, F. (2008). Mirdita Zone ophiolites and associated sediments in Albania reveal Neotethys Ocean origin. *International Journal Earth Science*, *97*, 865–881.

Gawlick, H.-J., Frisch, W., Vecsei, A., Steiger, T., & Böhm, F. (1999). The change from rifting to thrusting in the Northern Calcareous Alps as recorded in Jurassic sediments. *Geologische Rundschau*, *87*, 644–657.

Gawlick, H.-J., Krystyn, L., & Lein, R. (1994). Conodont colour alteration indices: Paleotemperatures and metamorphism in the Northern Calcareous Alps—A general view. *Geologische Rundschau*, *83*, 660–664.

Gawlick, H.-J., Lein, R., Missoni, S., Krystyn, L., Frisch, W., & Hoxha, L. (2014). The radiolaritic-argillaceous Kcira-Dushi-Komani sub ophiolitic Hallstatt Mélange in the Mirdita Zone of northern Albania. *Buletini I Shkencave Gjeologjike*, *4*, 1–32.

Gawlick, H.-J., & Missoni, S. (2015). Middle Triassic radiolarite pebbles in the Middle Jurassic Hallstatt Mélange of the Eastern Alps: Implications for Triassic Jurassic geodynamic and palaeogeographic reconstructions of the western Tethyan realm. *Facies*, *61*, 1–19.

Gawlick, H.-J., & Missoni, S. (2019). Middle-Late Jurassic sedimentary mélange formation related to ophiolite obduction in the Alpine-Carpathian-Dinaridic Mountain Range. *Gondwana Research*, *74*, 144–172.

Gawlick, H.-J., Missoni, S., Goričan, S., & Lein, R. (2012a). Late Anisian platform drowning and radiolarite deposition as a consequence of the opening of the Neotethys Ocean (High Karst Nappe, Montenegro). *Bulletin de la Societe Geologique de France*, *183*(4), 349–358.

Gawlick, H.-J., Missoni, S., Schlagintweit, F., & Suzuki, H. (2012b). Jurassic active continental margin deep-water basin and carbonate platform formation in the north-western Tethyan realm (Austria, Germany). *Journal of Alpine Geology*, *54*, 189–291.

Gawlick, H.-J., Missoni, S., Schlagintweit, F., Suzuki, H., Frisch, W., Krystyn, L., Blau, J., & Lein, R. (2009). Jurassic Tectonostratigraphy of the Austroalpine domain. *Journal of Alpine Geology*, *50*, 1–152.

Gawlick, H.-J., Missoni, S., Sudar, M. N., Gorican, S., Lein, R., & Stanzel, A. I. (2017). Open-marine Hallstatt Limestones reworked in the Jurassic Zlatar Mélange (SW Serbia): A contribution to understanding the orogenic evolution of the Inner Dinarides. *Facies*, *63*(29), 25.

Gawlick, H.-J., Missoni, S., Suzuki, H., Sudar, M., Lein, R., & Jovanović, D. (2016). Triassic radiolarite and carbonate components from the Jurassic ophiolitic mélange (Dinaridic Ophiolite Belt). *Swiss Journal of Geosciences*, *109*(3), 473–494.

Gawlick, H.-J., Schlagintweit, F., & Suzuki, H. (2007). Die Ober-Jura bis Unter-Kreide Schichtfolge des Gebietes Sandling-Höherstein (Salzkammergut, Österreich)—Implikationen zur Rekonstruktion des Block Puzzles der zentralen Nördlichen Kalkalpen, der Gliederung der karbonatklastischen Radiolaritflyschbecken und der Entwicklung der Plassen Karbonatplattform. *Neues Jahrbuch Geologisch Paläontologische Abhandlungen*, *243*, 1–70.

Gawlick, H.-J., Sudar, M., Lein, R., Missoni, S., Jovanović, D., & Suzuki, H. (2010). The Hallstatt Mélange occurrence of Vodena Poljana in the Inner Dinarids (Zlatar Mountain, SW Serbia). *Journal of Alpine Geology*, *52*, 116–118.

Gawlick, H.-J., Suzuki, H., & Missoni, S. (2001). Nachweis von unterliassischen Beckensedimenten in Hallstätter Fazies (Dürrnberg Formation) im Bereich der Hallein-Berchtesgadener Hallstätter Zone und des Lammer Beckens (Hettangium–Sinemurium). *Mitt. Ges. Geol. Bergbaustud. Österr.*, *45*, 39–55.

Goričan, Halamić, J., Grgasović, T., & Kolar-Jurkovšek, T. (2005). Stratigraphic evolution of Triassic arc-backarc system in northwestern Croatia. *Bull Soc Geol France*, *176*(1), 3–22.

Goričan, S., & Buser, S. (1989). Middle Triassic radiolarians from Slovenia (Yugoslavia). *Geologija*, *31*(32), 133–197.

Grecula, P., Kobulský, J., Gazdačko, L., Németh, Z., & Hraško, L. (2009). Geological Map of the Spiš-Gemer Ore Mts. 1:50,000. Grecula P, editor. *Ministry of the Environment of the Slovak Republic. Bratislava: State Geological Institute of Dionýz Štúr*.

Gümbel, C. W. (1891). Geognostische Beschreibung der Fränkischen Alb (Frankenjura) mit dem anstoßenden fränkischen Keupergebiete. *Kassel (T. Fischer)*, 1–763.

Haas, J., & Kovács, S. (2012). Pelso composite unit. In: Haas, J. (Ed.), Geology of Hungary. *Springer*, 21–80.

Haas, J., Kovács, S., Gawlick, H.-J., Gradinaru, E., Karamata, S., Sudar, M., Péró, Cs., Mello, J., Polák, M., Ogorelec, B., & Buser, S. (2011). Jurassic evolution of the tectonostratigraphic units of the Circum-Pannonian Region. *Jahrbuch der Geologischen Bundesanstalt*, *151*, 281–354.

Haas, J., Kovács, S., Krystyn, L., & Lein, R. (1995). Significance of Late Permian Triassic facies zones in terrane reconstructions in the Alpine North Pannonian domain. *Tectonophysics*, *242*, 19–40.

Hahn, F. (1913). Grundzüge des Baus der nördlichen Kalkalpen zwischen Inn und Enns. *Mitt. Geol. Ges. Wien*, *6*, 238–357 and 374–501.

Handy, M. R., Ustaszewski, K., & Kiessling, E. (2015). Reconstructing the Alps Carpathians- Dinarides as a key to understanding switches in subduction polarity, slab gaps and surface motion. *International Journal Earth Science*, *104*, 1–26.

Haug, É., & Lugeon, M. (1904). Sur l`éxistence dans le Salzkammergut de quatre nappes de charriage superposés. *C R Acad Sci*, *139*, 892–894.

Ivan, P.-. (2002). Relics of the Meliata Ocean crust: Geodynamic implications of mineralogical, petrological, and geochemical proxies. *Geologica Carpathica*, *53*, 245–256.

Kamenický, J. (1957). Serpentinity a diabázové horniny triasu okokua Jakliviec. *Geol. Práce Zos. (Bratislava)*, *46*, 3–71.

Kober, L. (1912). Der Deckenbau der östlichen Nordalpen. *Denkschr. österr. Akad. Wiss., math.-nat., Wien*, *88*.

Kovács, S., Ozsvart, P., Palinkas, L. A., Kiss, G., Molnar, F., Jozsa, S., & Köver, S. (2010). Re-evaluation of the Mesozoic complexes of Darno Hill (NE Hungary) and comparisons with Neotethyan accretionary complexes of the Dinarides and Hellenides – prelimary data. *Central European Geology*, *53*, 205–231.

Kovács, S., Polák, M., Aljinović, D., Ogorelec, B., Kolar-Jurkovšek, T., Jurkovšek, B., & Buser, S. (2011). Triassic evolution of the tectonostratigraphic units of the Circum- Pannonian Region. *Jahrbuch der Geologischen Bundesanstalt*, *151*, 199–280.

Kozur, H. (1988). Muelleritortiidae n. Fam., eine charakteristische longobardische (oberladinische) Radiolarienfamilie, Teil 1. *Freiberger Forsch.-H.*, 51–61.

Kozur, H. (1991). The evolution of the Meliata Hallstatt Ocean and its significance for the early evolution of the Eastern Alps and Western Carpathians. *Palaeogeogr Palaeoclimatol Palaeoecol*, *87*, 109–135.

Kozur, H., & Mock, R. (1985). Erster Nachweis von Jura in der Meliata-Einheit der südlichen Westkarpaten. *Geol. Paläont. Mitt. Innsbruck*, *13*(10), 223–238.

Kozur, H., & Mock, R. (1995). New palaeogeographic and tectonic interpretations in the Slovakian Carpathians and their implications for correlations with the Eastern Alps. Part I: Central Western Carpathians. *Mineralia Slovaca*, *28*, 151–174.

Kozur, H., & Mock, R. (1997). New paleogeographic and tectonic interpretations in the Slovakian Carpathians and their implications for correlations with the Eastern Alps and other parts of the Western Tethys. Part II: Inner Western Carpathians. *Mineralia Slovaca*, *29*, 164–209.

Kozur, H., Mock, R., & Ožvoldová, L. (1996). New biostratigraphic results in the Meliaticumin its type area around Meliata village (Slovakia) and their tectonic and paleogeographic significance. *Geologisch Paläontologische Mitteilungen Innsbruck*, *21*, 89–121.

Kozur, H., & Mostler, H. (1992). Erster paläontologischer Nachweis von Meliaticum und Süd-Rudabányaicum in den Nördlichen Kalkalpen (Österreich) und ihre Beziehungen zu den Abfolgen in den Westkarpaten. *Geologisch Paläontologische Mitteilungen Innsbruck*, *18*, 87–129.

Kraus, E. (1944). Über den Flysch und den Kalkalpenbau von Oberdonau. *Jb. Ver. f. Landeskunde u. Heimatpflege, Linz*, *91*.

Krystyn, L. (2008). The Hallstatt pelagics – Norian and Rhaetian Fossillagerstaetten of Hallstatt. *Berichte der Geologischen Bundesanstalt Wien*, *76*, 81–98.

Kukoč, D., Gorican, S., & Kosir, A. (2012). Lower cretaceous carbonate gravity-flow deposits fromBohinj area (NWSlovenia): Evidence of a lost carbonate platformin the Internal Dinarides. *Bulletin de la Société géologique de France*, *183*, 383–392.

Lein, R., & Gawlick, H.-J. (2008). Plattform-Drowning im mittleren Anis-ein überregionaler Event. *Journal of Alpine Geology*, *49*, 61–62.

Leško, B., & Varga, I. (1980). Alpine elements in the West Carpathian structure and their significance. *Mineralia Slovakia*, *12*, 97–130.

Mahel, M. (1986). Geological Structure of the Czechoslovak Carpathians. Paleoalpine units. *Veda*, *486*.

Maluski, H., Rajlich, P., & Matte, P. (1993). 40Ar/39Ar dating of the Inner Carpathians Variscan basement and Alpine mylonitic overprinting. *Tectonophysics*, *223*, 313–337.

Mandl, G. W. (1984). Zur Trias des Hallstätter Faziesraumes-ein Modell am Beispiel Salzkammergut (Nördliche Kalkalpen, Österreich). *Mitt. Ges. Geol. Bergbaustud. Österr.*, *30/31*, 133–176.

Mandl, G. W. (1996). Zur Geologie des Ödenhof Fensters (Nördliche Kalkalpen, Österreich). *Jahrbuch der Geologischen Bundesanstalt*, *139*, 473–495.

Mandl, G. W., & Ondrejičková, A. (1991). Über eine triadische Tiefwasserfazies (Radiolarite, Tonschiefer) in den Nördlichen Kalkalpen—Ein Vorbericht. *Jahrbuch der Geologischen Bundesanstalt*, *134*, 309–318.

Mandl, G. W., & Ondrejičková, A. (1993). Radiolarien und Conodonten aus dem Meliatikum im Ostabschnitt der Nördlichen Kalkalpen (Österreich). *Jahrbuch der Geologischen Bundesanstalt*, *136*, 841–871.

Mello, J., Elecko, M., Pristas, J., Reichwalder, P., Snopko, L., Vass, D., Vozarova, A., Gaal, L., Hanzel, V., Hok, J., Slavkay, M., & Steiner, A. (1997). Vysvetlivky ku geologickej mape Slovenskeho krasu 1:50000. *GSSR, Bratislava*, *256*.

Mello, J., Reichwalder, P., & Vozarova, A. (1998). Borka Nappe: High pressure relic from the subduction-accretion prism of the Meliata ocean (Inner Western Carpathians, Slovakia). *Slovak Geologica Magazine*, *4*, 161–273.

Meschede, M. (1986). A method of discrimination between different types of mid ocean ridge basalts and continental tholeiites with the Nb–Zr–Y diagram. *Chemical Geology*, *56*, 207–218.

Missoni, S., & Gawlick, H.-J. (2011a). Evidence for Jurassic subduction from the Northern Calcareous Alps (Berchtesgaden; Austroalpine, Germany). *International Journal of Earth Science*, *100*, 1605–1631.

Missoni, S., & Gawlick, H.-J. (2011b). Jurassic mountain building and Mesozoic-Cenozoic geodynamic evolution of the Northern Calcareous Alps as proven in the Berchtesgaden Alps (Germany). *Facies*, *57*, 137–186.

Mock, R. (1980). Triassic of the West Carpathians. *Abhandlungen der Geologischen Bundesanstalt*, *35*, 129–144.

Mock, R., Sýkora, M., Aubrecht, R., Ozvoldová, L., & Kronome, B. (1998). Petrology and petrography of the Meliaticum near the Meliata and Jaklovce villages, Slovakia. *Slovak Geological Magazine*, *4*, 223–260.

Mosher, L. C. (1968). Triassic conodonts from western North America and Europe and their correlation. *Journ. Pale-ont., Larvrence Kansas*, *42*, 895–946.

Mostler, E. (1967). Conodonten und Holothuriensklerite aus den norishen Hallstatter-Kalken von Hernstein (Niederoesterreich). *Geol. B.-A., Wien*, 177–188.

Neubauer, F., Friedl, G., Genser, J., Handler, R., Mader, D., & Schneider, D. (2007). Origin and tectonic evolution of the Eastern Alps deduced from dating of detrital white mica: A review. *Austrian Journal Earth Sciences*, *100*, 8–23.

Nitra, G., Aberhan, M., Bortolotti, V., Carras, N., Menna, F., & Fazzuoli, M. (2020). Deciphering the geodynamic evolution of the Dinaric orogen through the study of the 'overstepping' Cretaceous successions. *Geological Magazine*, *157*(8), 1238–1264.

Nowak, J. (1911). Über den Bau der Kalkalpen in Salzburg und im Salzkammergut. *Acad Sci Cracovie Bull*, *911*, 57–196.

Ozsvart, P., Dosztaly, L., Migiros, G., Tselepidis, V., & Kovacs, S. (2012). New radiolarian biostratigraphic age constraints on Middle Triassic basalts and radiolarites from the Inner Hellenides (Northern Pindos and Othris Mountains, Northern Greece) and their implications for the geodynamic evolution of the early Mesozoic Neotethys. *International Journal Earth Sciences*, *101*, 1487–1501.

Ozsvart, P., & Kovács, S. (2012). Revised Middle and late Triassic radiolarian ages for ophiolite mélanges: Implications for the geodynamic evolution of the northern part of the early Mesozoic Neotethyan subbasins. *Bulletin de la Société géologique de France*, *183*, 273–286.

Pamic, J. (1984). Triassic magmatism of the Dinarides in Yugoslavia. *Tectonophysics*, *109*, 273–307.

Pantanelli, D. (1980). I diaspri della Toscana e i loro fossili: Atti della Reale Accademia dei Lincei. *Classe di Scienze Fisiche, Matematiche e Scienze Naturali, ser. 3*, *8*, 35–66.

Piller, W. E., Egger, H., Erhart, C. W., Gross, M., Harzhauser, M., Hubmann, B., Van Husen, D., Krenmayr, H. G., Krystyn, L., Lein, R., Lukeneder, A., Mandl, G. W., Rögl, F., Roetzel, R., Rupp, C., Schnabel, W., Schönlaub, H. P., Summesberger, H., Wagreich, M., & Wessely, G. (2004). Die stratigraphische Tabelle von Österreich 2004 (sedimentäre Schichtfolgen). *Österreichische Akademie der Wissenschaften und Österreichische Stratigraphische Kommission, Wien*.

Plašienka, D. (2012). Jurassic syn-rift and Cretaceous syn-orogenic, coarse-grained deposits related to opening and closure of the Vahic (South Penninic) Ocean in the Western Carpathians – an overview. *Geological Quarterly*, *56*, 601–628.

Plašienka, D. (2018). Continuity and Episodicity in the Early Alpine Tectonic Evolution of the Western Carpathians: How Large-Scale Processes Are Expressed by the Orogenic Architecture and Rock Record Data. *Tectonics*, *37*, 2029–2079.

Plašienka, D., Grecula, P., Putiš, M., Kováč, M., & Hovorka, D. (1997). Evolution and structure of the Western Carpathians: An overview. *Bratislava: Mineralia Slovaca*, 1–24.

Plöchinger, B., & Prey, S. (1968). Profile durch die Windischgarstener Störungszone im Raume Windischgarsten-St. Gallen. *Jb. Geol. B.-A*, *111*, 175–211.

Putiš, M. (2020). Origin and Age Determination of the Neotethys Meliata Basin Ophiolite Fragments in the Late Jurassic-Early Cretaceous Accretionary Wedge Mélange (Inner Western Carpathians, Slovakia). *Minerals*, *9*(11), 652.

Putiš, M., Soták, J., Li, Q. L., Ondrejka, M., Li, X. H., Hu, Z., Ling, X., Nemec, O., Németh, Z., & Ružicka, P. (2019). Origin and Age Determination of the Neotethys Meliata Basin Ophiolite Fragments in the Late Jurassic–Early Cretaceous Accretionary Wedge Mélange (Inner Western Carpathians, Slovakia). *Minerals*, *9*(11), 652.

Ricou, L.-E. (1995). The plate tectonic history of the past Tethys ocean. *The Tethys ocean. Springer, Boston*, 3–70.

Robertson, A. H. F. (2012). Late Palaeozoic-Cenozoic tectonic development of Greece and Albania in the context of alternative reconstructions of Tethys in the Eastern Mediterranean region. *International Geology Review*, *54*, 373–454.

Schlager, W., & Schöllnberger, W. (1974). Das Prinzip stratigraphischer Wenden in der Schichtfolge der Nördlichen Kalkalpen. *Mitt. Geol. Ges. Wien*, *66*(67), 165–193.

Schlagintweit, F., & Gawlick, H.-J. (2007). Analysis of Late Jurassic to Early Cretaceous algal debris facies of the Plassen carbonate platform in the Northern Calcareous Alps (Germany, Austria) and in the Kurbnesh area of the Mirdita zone (Albania): A tool to reconstruct tectonics and palaeogeography of eroded platforms. *Facies*, *53*, 209–227.

Schlagintweit, F., & Gawlick, H.-J. (2009). Lituola? Baculiformis n. Sp., a new benthic foraminifer from Late Jurassic perireefal carbonates of the Western Tethyan domain. *Journal of Alpine Geology*, *51*, 39–49.

Schlagintweit, F., Gawlick, H.-J., Missoni, S., Hoxha, L., Lein, R., & Frisch, W. (2008). The eroded Late Jurassic Kurbnesh carbonate platform in the Mirdita Ophiolite Zone of Albania and its bearing on the Jurassic orogeny of the Neotethys realm. *Swiss Journal of Geosciences*, *101*, 125–138.

Schmid, S. M., Bernoulli, D., Fügenschuh, B., Matenco, B., Schefer, S., Schuster, R., Tischler, M., & Ustaszewski, K. (2008). The Alpine-Carpathian-Dinaride-orogenic system: Correlation and evolution of tectonic units. *Swiss Journal of Geosciences*, *101*, 139–183.

Schmid, S. M., Fügenschuh, B., Kounov, A., Matenco, L., Nievergelt, P., Oberhänsli, R., Pleuger, J., Schefer, S., Schuster, R., Tomljenovic, B., Ustaszewski, K., & van Hinsbergen, DJJ. (2020). Tectonic units of the Alpine collision zone between Eastern Alps and western Turkey. *Gondwana Res*, *78*, 308–374.

Şengör, A. M. C. (1985). Die Alpiden und die Kimmeriden: Die verdoppelte Geschichte der Tethys. *Geologische Rundschau*, *74*, 181–213.

Şengör, A. M. C. (1997). Asia. In: Moores, E., Fairbridge, E. (Eds.), Encyclopedia of Europaean and Asian Regional Geology. *Chapman & Hall, London*, 34–51.

Şengör, A. M. C. (2015). Eduard Suess and Global Tectonics: An illustrated “Short Guide”. *Austrian Journal of Earth Sciences*, *107*, 6–82.

Septfontaine, M. (1977). Niveaux à Foraminifères (Pfenderininae et Valvulininae) dans le Dogger des Préalpes médianes du Chablais occidental Haute-Savoie, France). *Ecologae geol. Helv., Basel*, *70*, 599–635.

Spengler, E. (1919). Die Gebirgsgruppe des Plassen und Hallstätter Salzberges im Salzkammergut. *Jahrb. Geol. Reichsanst.*, *68*, 285–474.

Spengler, E. (1959). Versuch einer Rekonstruktion des Ablagerungsraumes der Decken der Nördlichen Kalkalpen. III. Tl.: Der Ostabschnitt der Kalkalpen. *Jb. Geol. B.-A, Wien*, *102*(2).

Stampfli, G. M., & Kozur, H. W. (2006). Europe from Variscan to the Alpine cycles. *Memoirs-Geological Society of London*, *32*, 57–82.

Steinmann, G. (1925). Gibt es fossile Tiefseeablagerungen von erdgeschichtlicher Bedeutung? *Geologische Rundschau*, *16*, 435–468.

Steinmann, G. (1927). Die ophiolitischen Zonen in den mediterranen Kettengebirgen: *Compte-rendu, XIVe Congrès Géologique International*, *2*, 637–667.

Sudar, M., Gawlick, H.-J., Lein, R., Missoni, S., Kovács, S., & Jovanović, D. (2013). Depositional environment, age and facies of the Middle Triassic Bulog and Rid formations in the Inner Dinarides (Zlatibor Mountain, SW Serbia): Evidence for the Anisian break-up of the Neotethys Ocean. *Neues Jahrbuch Geologisch Paläontologische Abhandlungen*, *269*, 291–320.

Sudar, M., Gawlick, H.-J., Missoni, S., Jovanović, D., & Lein, R. (2015). The Middle Triassic (Anisian) Bulog Formation in the Dinarides: Definition, use and reality. New insights from new and revised sections in the Dinarides (Dinaridic Ophiolite Belt, Serbia). *2nd International Congress on Stratigraphy*, 19–23.

Sudar, M., Gawlick, H.-J., Missoni, S., Suzuki, H., Jovanović, D., & Lein, R. (2010). The carbonate clastic radiolaritic mélange of Pavlovica Cuprija: A key to solve the palaeogeography of the Hallstatt Limestones in the Zlatar Mountain (SW Serbia). *Journal of Alpine Geology*, *52*, 53–57.

Suess, E. (1901). *Abschieds-Vorlesung. Beitrage zur Paläontologie und Geologie Gesellschaft Österreich-Ungarns und des Orient*. *14*, 2–8.

Sun, S. S., & McDonough, WF. (1989). Chemical and isotopic systematics of oceanic basalts: Implications for mantle composition and processes. *Geological Society London Special Publications*, *42*, 313–345.

Sun, S. S., Robert, W. N., & Anatoly, Y. S. (1979). Geochemical Characteristics of Mid-Ocean ridge basalts. *Earth and Planetary Science Letters*, *44*(1), 119–138.

Tekin, U. K. (1999). Biostratigraphy and Systematics of late Middle to Late Triassic radiolarians from the Taurus Mountains and Ankara region, Turkey. *Geol. Paläont. Mitt. Innsbruck, Sonderband*, *5*, 1–297.

Thalmann, H. E. (1951). Mitteilungen über Foraminiferen IX. *Ecologae geol. Helv., Basel*, *43*, 221–225.

Tollmann, A. (1962). Die Baustile in den tektonischen Einheiten der Nördlichen Kalkalpen. *Z. Deutsch, geol. Ges., Hannover*, *113*.

Tollmann, A. (1963). Hundert Jahre Geologisches Institut der Universität Wien. *Gesellschaft der Geologie und Bergbaustudien*.

Tollmann, A. (1985). *Geologie von Österreich, Band 2: Außerzentralalpiner Anteil*. 1–710.

Tollmann, A. (1987). Late Jurassic/Neogene Gravitational Tectonics in the Northern Calcareous Alps in Austria. *-(In: Flügel, H.W. & Faupl, P. (Eds.): Geodynamics of the Eastern Alps)*, 112–125.

Weynschenk, R. (1950). Die Jura-Mikrofauna und –flora des Sonnwendgebirges (Tirol). - Schlern—Schriften. *Universität Innsbruck*, *83*, 1–32.

Wood, DA. (1980). The application of a Th-Hf-Ta diagram to problems of tectonomagmatic classification and to establishing the nature of crustal contamination of basaltic lavas of the British Tertiary volcanic province. *Earth and Planetary Science Letters*, *50*, 11–30.